

## Gallol containing adhesive polymers

Sundol Kim<sup>†</sup>, Biswajit Saha<sup>†</sup>, Jacob Boykin<sup>†</sup>, and Hoyong Chung

Department of Chemical and Biomedical Engineering, FAMU-FSU College of Engineering, Tallahassee, FL, USA

### ABSTRACT

The gallol group, which contains three adjacent hydroxyl groups on a benzene, is a new bioinspired functional group for adhesives applications. The chemical structure of the gallol group possesses one more hydroxyl group on a benzene than the well-studied mussel-inspired adhesive group, catechol. Despite the small difference in chemical structure, gallol containing adhesive polymers show 7 times higher wet adhesion properties than the catechol containing adhesives under the identical experimental conditions. On account of the large enhancement of adhesion properties, the gallol containing adhesive polymers are gaining significant interest, and the related polymer science fields are expected to grow quickly. This review summarizes synthesis methods and diverse applications of gallol containing adhesive polymers. The goal of this review is to provide reasonable pathways for selecting and designing gallol containing polymer structures to maximize the adhesion properties for functional applications.

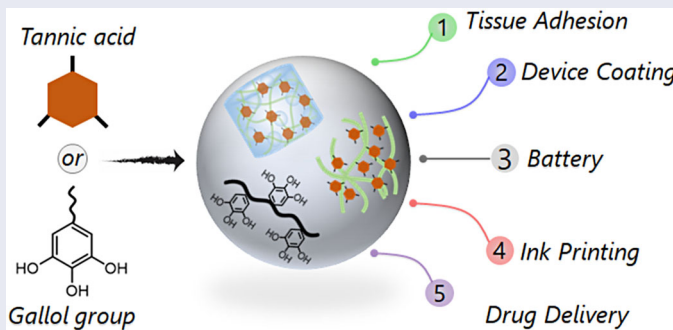
### ARTICLE HISTORY

Received May 2022  
Accepted June 2022

### KEYWORDS

Adhesives; battery;  
bioinspired polymer;  
biomedical adhesives;  
coating; drug delivery;  
gallol; hydrogel; polymer  
synthesis; 3D printing

### GRAPHICAL ABSTRACT



## 1. Introduction

The most extensively studied bioinspired adhesives are catechol containing polymers. The catechol is found from L-3,4-dihydroxyphenylalanine (DOPA) which is an integral part of mussel's adhesive protein. Because of the DOPA containing polymer's excellent adhesion properties on universal surfaces, research regarding the bioinspired (or mussel-inspired) adhesives has been extensively studied and reviewed many times.<sup>[1-5]</sup> However, gallol, which has one more hydroxyl group on a benzene ring than catechol (Figure 1), has not been reviewed yet despite gallol's much stronger adhesion properties than catechol group. The present review focuses on "adhesive polymers" and discusses comparison between gallol and catechol in adhesive polymers, synthesis of gallol containing adhesive polymers, and applications of gallol containing adhesive polymers.

Gallol possesses three adjacent hydroxyl groups on a benzene ring, and it is commonly found in a variety of plants

such as tea leaves, fruit peels, and oak bark.<sup>[6,7]</sup> The simplest compound of gallol containing group is pyrogallol, which is extracted from gallic acid. Tannic acid, known as a bitter element in red wine,<sup>[8,9]</sup> is also a gallol group containing molecule (Figure 2).<sup>[10]</sup>

The unique chemical structure of gallol group has been applied to multiple areas in polymer science. First, integration of gallol on polymers can significantly improve adhesion properties on universal surfaces. This is a main theme of the present review. Among diverse gallol containing adhesives, strong gallol adhesion on proteins, peptides, DNA/RNA, and polysaccharides gains heightened attention in the biomedical adhesives field.<sup>[11,12]</sup> The gallol groups containing polymers are an excellent antioxidant.<sup>[13]</sup> The antioxidant function is enabled by quinone, that is obtained from oxidation of hydroxyl groups on gallol under physiological and weak basic conditions. The next application area uses gallol to form transition metal complex via coordination bonds. This metal complexation leads strong attraction

between metal (surface, micro/nano particles, and atomic metals) and coating polymers in engineering processes.<sup>[14]</sup>

### 1.2. Gallo group versus catechol group

The main difference of chemical structure between gallo groups and catechol group is the number of hydroxyl groups on a benzene ring (3 on gallo vs. 2 on catechol). Three hydroxyl groups of gallo group are attached to 3, 4, and 5 position on a phenyl group. On the other hand, catechol possesses two hydroxyl groups on 3 and 4 positions of a phenyl group (Figure 1). The chemical structure difference does not seem significant; however, the resulting properties and the following application difference are significant. Recently, comparative underwater adhesion property studies of catechol and gallo are reported in 2017 by Yoshie et al.<sup>[15]</sup> In this report, the synthesized poly(vinylgallo-co-*n*-butyl acrylate) showed 1 MPa of bonding strength on

aluminum substrate under water after 6 days curing. It is almost 7 times stronger than bonding strength of poly(vinylcatechol-co-*n*-butyl acrylate) which replaces gallo groups in polymer with catechol under same conditions (Figure 3).<sup>[15]</sup> The gallo containing polymer also showed much higher bonding strength than catechol group containing polymer under seawater, PBS solution, and the air. The detailed discussion of Yoshie et al.'s paper is shown in "2-1. Covalently linked pendant gallo" in this review with presenting synthesis methods and property test results.

In 2021, Lee et al.<sup>[16]</sup> reported a comparative study with catechol modified polyallylamine (PAA-CA) and gallo modified polyallylamine (PAA-GA) as shown in Figure 4a. In this report, the gallo group containing materials showed enhanced mechanical properties than that of the catechol group containing materials such as storage modulus and compressive strength. In addition, the adhesion strength on tissue of gallo modified polymer is almost twice that of catechol. Furthermore, comparative studies of self-healing properties, antioxidant properties, and adhesive properties are investigated in this report. PAA-GA showed (1) 116% enhanced self-healing ability due to more effective reversible formation of imine bonds by the gallo group, and (2) 150% enhanced antioxidant activities because more hydroxyl groups from gallo group can scavenge more radicals and provide more electrons to free radical (Figure 4b-d).<sup>[16]</sup> A similar trend was also reported by Zhan et al.<sup>[17]</sup> In this report, polyvinyl gallo showed 200% enhanced antioxidant ability than that of polyvinyl catechol.

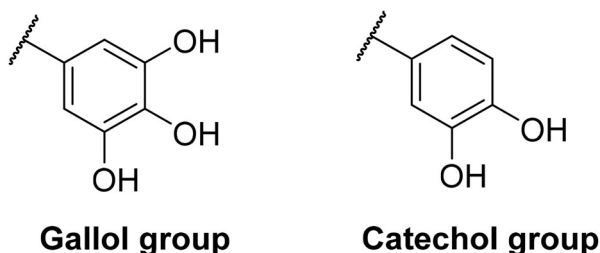


Figure 1. Chemical structure of gallo and catechol group.

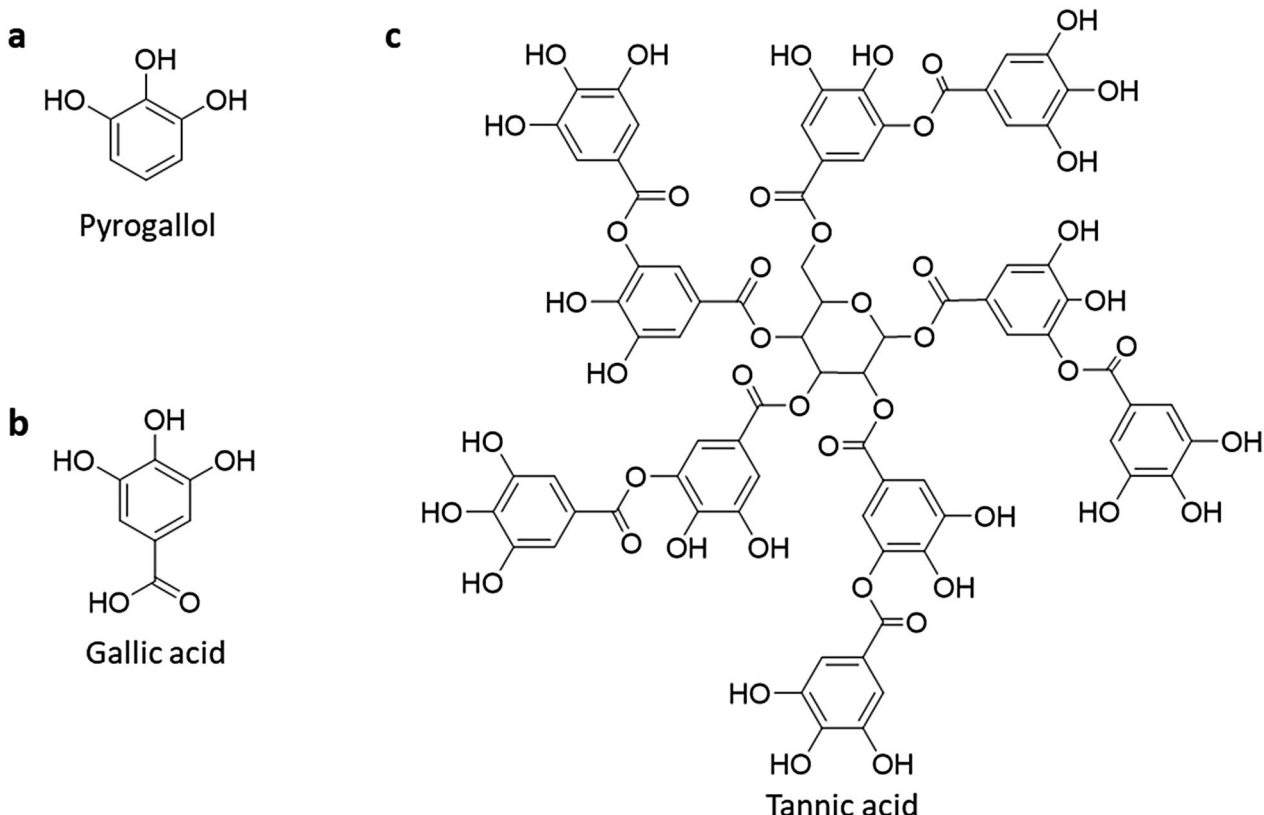
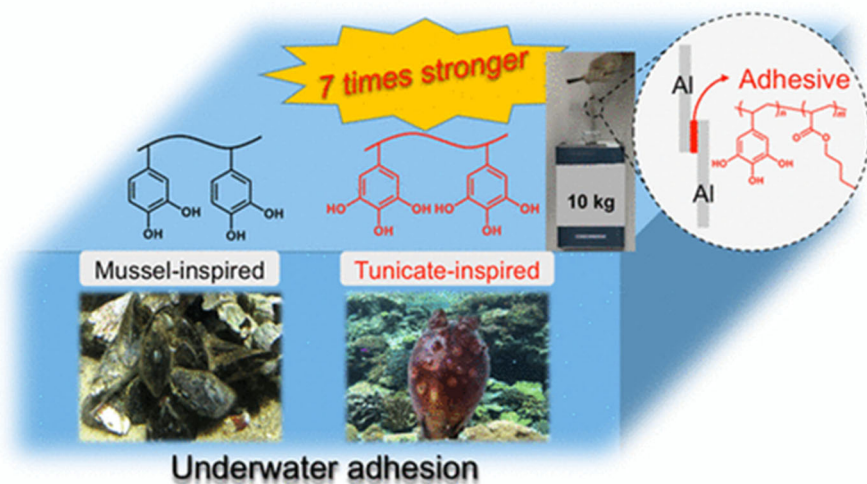
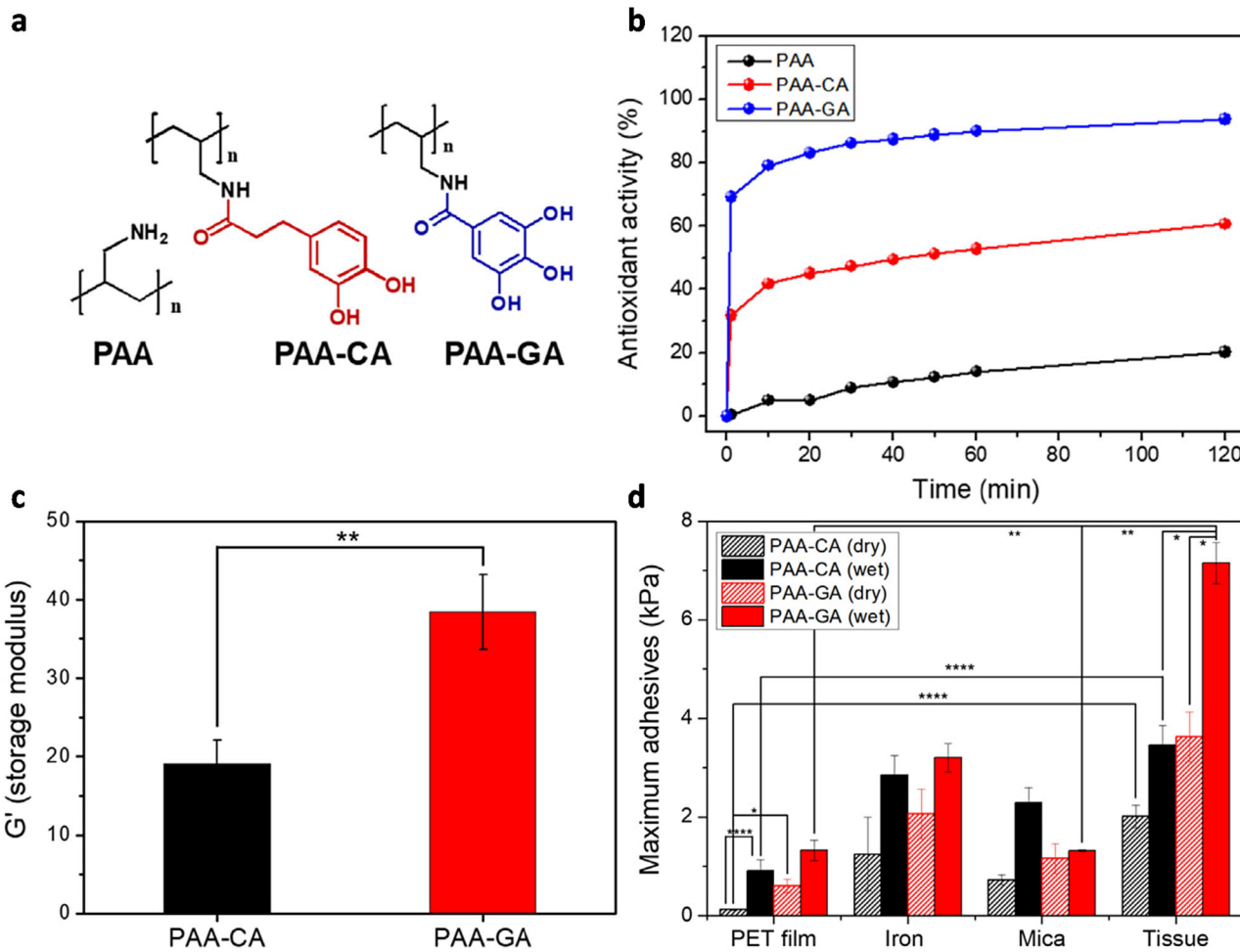


Figure 2. Chemical structures of well-known gallo containing compounds (a) pyrogallol, (b) gallic acid, and (c) tannic acid.



**Figure 3.** Comparison of adhesion strength between gallo and catechol under water. Reproduced with permission from ref. [15]. Copyright 2017, American Chemical Society.



**Figure 4.** (a) Chemical structure of PAA, PAA-CA, and PAA-GA. (b) Antioxidant activities of PAA, PAA-CA, and PAA-GA according to time. (c) Storage moduli (G) of PAA-CA and PAA-GA hydrogels at 1 rad/s frequency. (d) Maximum adhesive strengths of the PAA-CA and PAA-GA hydrogels on various substrates including the PET film, iron plate, mica plate, and porcine skin in dry and wet conditions. Reproduced with permission from ref [16]. Copyright 2021, Elsevier.

## 2. Design and syntheses

In general, the gallo-containing polymeric adhesives can be synthesized by various covalent bond forming chemical reactions and non-covalent interactions such as Schiff-base

reaction, Michael addition, sodium periodate mediated oxidation, hydrogen bonding, ionic interaction and so forth. The primary principle is to incorporate pyrogallol groups, including gallic acid (GA), tannic acid (TA), 3,4,5-trihydroxyphenylalanine (TOPA) into the polymeric systems. The

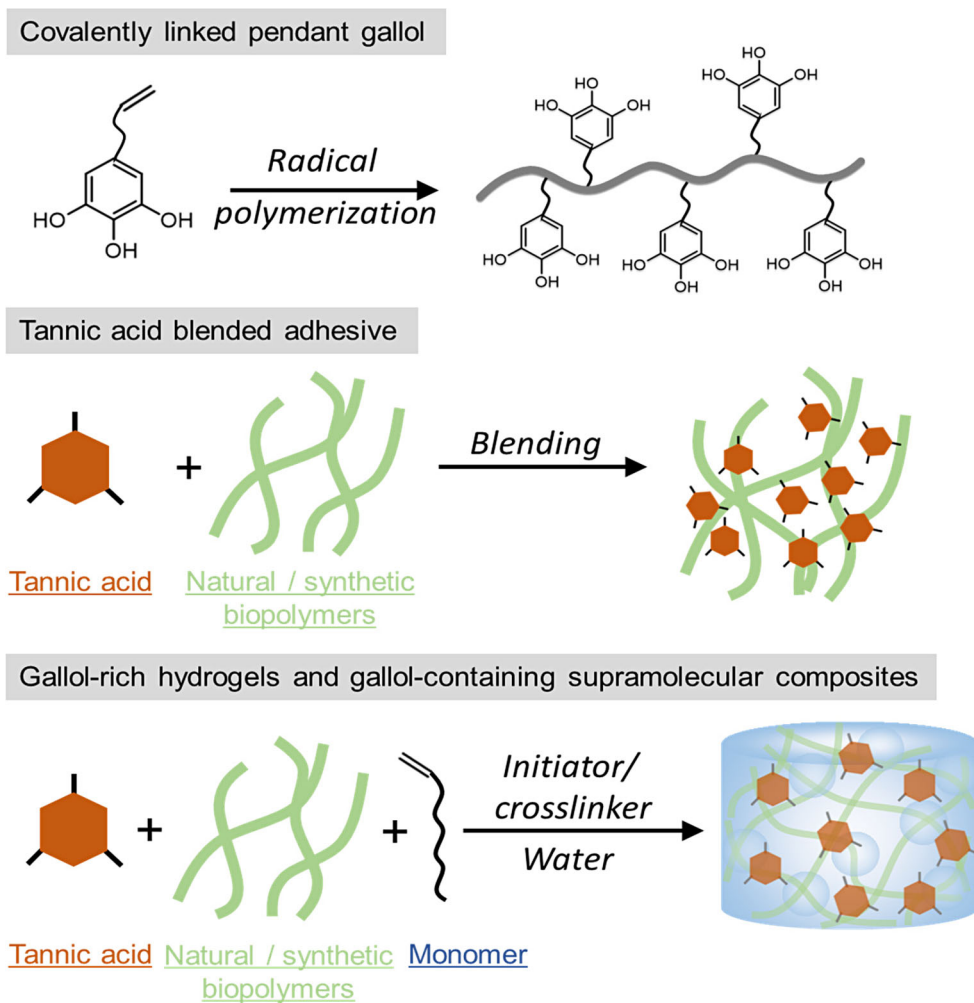


Figure 5. Three representative synthetic methods of gallol containing polymeric adhesives.

synthetic strategy toward gallol-based polymeric adhesives can be categorized into three groups: covalently linked pendant gallol, tannic acid blended adhesives, and gallol-rich hydrogels and gallol-containing supramolecular composites (Figure 5).

### 2.1. Covalently linked pendant gallol

Synthesis of gallol-containing vinyl monomers for radical polymerization is not trivial because of its radical scavenging behavior. Hence, a rational protection/deprotection strategy is necessary for high yield polymer synthesis. Initially, methoxy groups ( $-\text{OCH}_3$ ) have often been used for the protection of gallol,<sup>[17,18]</sup> but a harsh deprotection method requires boron tribromide ( $\text{BBr}_3$ )<sup>[19]</sup> that can easily cleave ether and ester linkages. In this regard, silyl protecting groups (e.g. *tert*-butyldimethylsilyl chloride (TBDMS)) have also been utilized.<sup>[20,21]</sup> However, the polymerization of TBDMS-protected gallol monomers resulted in an oligomer instead of polymer.

In this context, coworkers of Yoshie and Ejima introduced a new path toward the successful synthesis of homo and copolymers with pendant gallol moieties using methoxy-methyl protection, which can be deprotected by simple acid

treatment.<sup>[15,22]</sup> The monomer (vinylgallol, VGal, in Figure 6a) was synthesized through the protection of 3,4,5-trihydroxybenzaldehyde with chloromethyl methyl ether followed by the Wittig reaction with methyl triphenylphosphonium bromide ( $\text{Ph}_3\text{PCH}_3\text{Br}$ ) (Figure 6a). Homopolymer of VGal, PVGal, was too brittle to act as an adhesive. Nevertheless, the copolymer of VGal and *n*-butyl acrylate (BA), P(VGal-*co*-BA) synthesized *via* free radical polymerization (Figure 6b) exhibited strong adhesive performance under different environments: PBS ( $1.35 \pm 0.17$  MPa), water ( $1.01 \pm 0.26$  MPa) and seawater ( $1.34 \pm 0.43$  MPa). In comparison to catechol (P(VCat-*co*-BA)) and phenolic (P(VPh-*co*-BA)) copolymers, these gallol-containing copolymers showed better adhesive strength (seven times high in water). This fact has further proved the Bell theory<sup>[23,24]</sup>, which stated that bidentate interactions are more advantageous than monodentate. Moreover, P(VGal-*co*-BA) showed higher adhesive strength than commercially available isocyanate-based glue, Gorilla glue, in seawater ( $0.34 \pm 0.09$  MPa) and PBS ( $1.28 \pm 0.10$  MPa).

The wet adhesion performance of such gallol copolymers was further enhanced by incorporating styrene (St) instead of BA as a comonomer.<sup>[25]</sup> Because styrene can increase the cohesive interactions into the polymer *via*  $\pi$ - $\pi$  stacking. The underwater adhesion strength of P(VGal-*co*-St) on

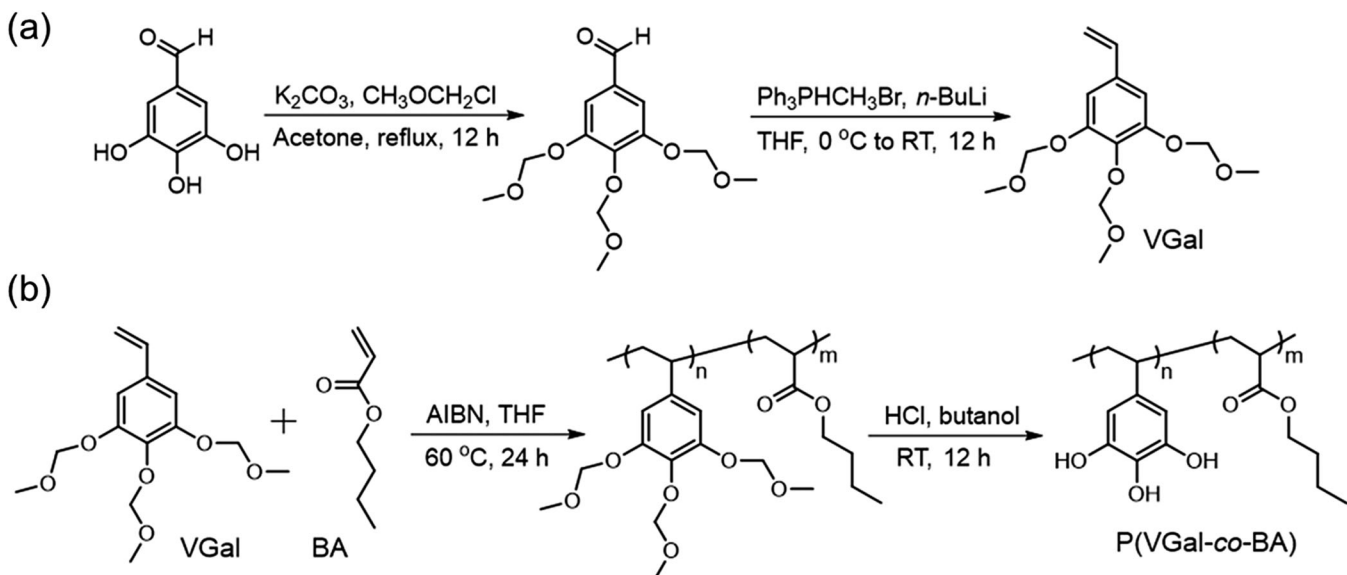


**Figure 6.** (a) Synthetic strategy adopted for the synthesis of vinylgallol (VGal) and (b) its copolymerization with BA. Adapted with permission from ref. [15]. Copyright 2017, American Chemical Society.

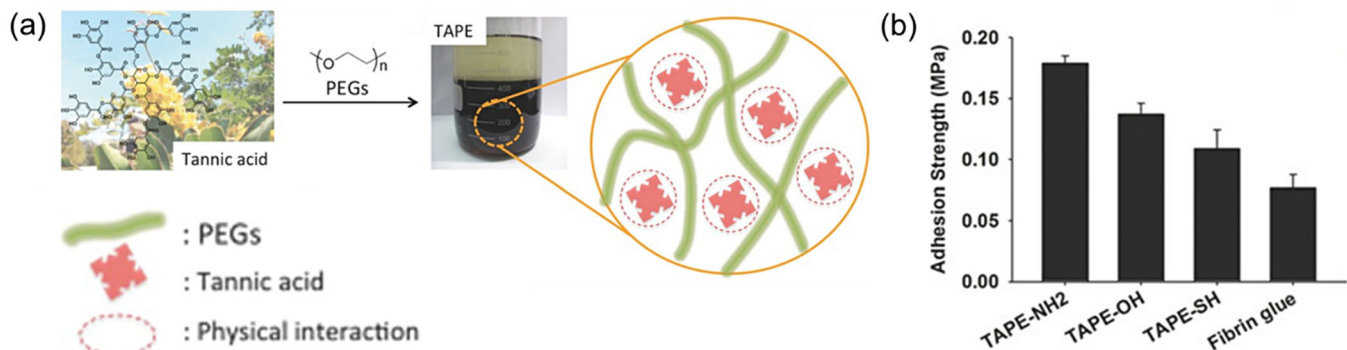


**Figure 7.** (a) Fabrication of TAPE by mixing TA and PEG. (b) Adhesion strengths analysis of TAPE containing different end functional groups ( $\text{NH}_2$ ,  $\text{OH}$ ,  $\text{SH}$ ) of PEG and fibrin glue. Reproduced with permission from ref. [29]. Copyright 2015, WILEY-VCH.

aluminum substrates, measured with both tensile and lap-shear tests, exceeded 4 MPa by optimizing the gallo content ( $\sim 10\%$ ) and molecular weight of the copolymer ( $M_n = 64\text{ kDa}$ ). Notably, an increment of the gallo content ( $> 10\%$ ) significantly reduces the adhesive strength due to the presence of fewer free gallo groups for surface interactions. However, the bonding strength remained unaltered on varying the molecular weight beyond 64 kDa. These aforesaid findings unequivocally suggest that the existence of a greater number of -OH groups are crucial for developing effective underwater adhesive systems. Although it is not related to an adhesive application, rationally designed gallo-containing norbornene monomers and their polymers were synthesized by ring-opening metathesis polymerization forming hydrogels<sup>[26]</sup> and gel-like solids.<sup>[27]</sup>

## 2.2. Tannic acid blended adhesives

Tannic acid (TA), a hydrolyzable derivative of tannin, ubiquitously found in plants.<sup>[28]</sup> It has a phenolic structure consisting of five outer-shell pyrogallol moieties that are covalently attached to inner -OH groups of five gallols (Figure 7a). TA has evolved into a popular polyphenol to

fabricate biomedical adhesives owing to its multifunctional properties, including antibacterial, anticarcinogenic, antimutagenic and antioxidant.<sup>[30,31]</sup> In addition, it possesses a strong binding affinity with various biomolecules, mainly proteins: elastin,<sup>[32]</sup> thrombin,<sup>[33]</sup> gelatin,<sup>[34]</sup> and synthetic polymers,<sup>[35,36]</sup> *viz.* poly(vinyl pyrrolidone), polyethylene glycol (PEG), and so on, *via* multidentate interactions (H-bonding).

Considering the unique facets of TA, Hong and Lee *et al.* presented the highly scalable medical adhesives (TAPE), prepared by simple mixing of TA and PEG at a 1:1 (w/w) concentration in distilled water in 2015 (Figure 7a).<sup>[29]</sup> TAPE exhibited much higher adhesiveness than each individual component, TA and PEG. Additionally, the adhesion strength of TAPE is substantially affected by varying the end groups and number of PEG arms. TAPE containing PEG-NH<sub>2</sub> (TAPE-NH<sub>2</sub>) displayed the highest adhesion strength ( $\sim 0.18\text{ MPa}$ ) on porcine skin, followed by TAPE-OH and TAPE-SH (Figure 7b). Most notably, in comparison to fibrin glue (0.07 MPa), TAPE-NH<sub>2</sub> showed 250% increase on the adhesion strength. Such superior adhesion originated from the interconnected robust molecular network formed by H-bonding between TA and ethylene glycol (EG) units of PEG.

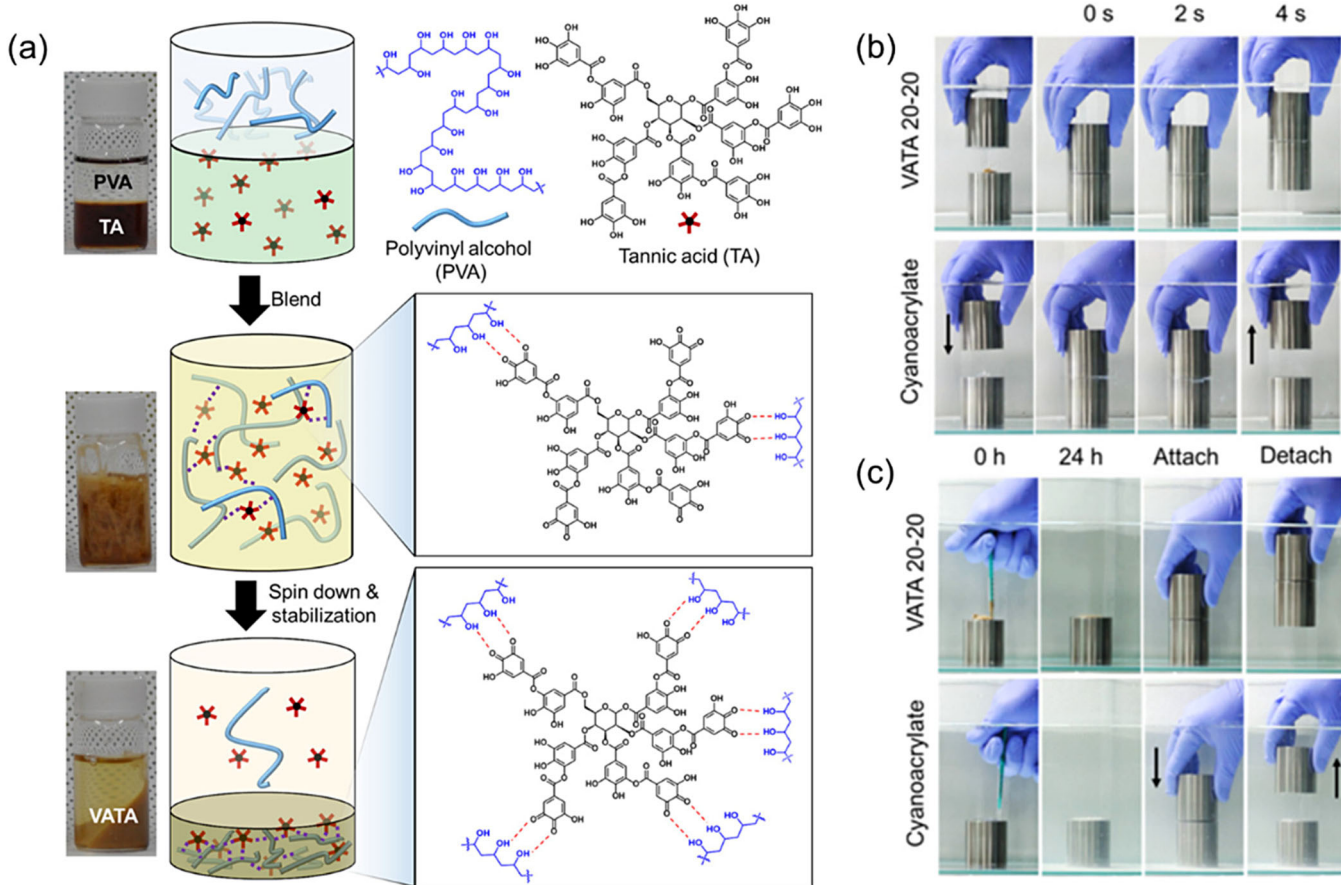


**Figure 8.** (a) Preparation of PVA and TA-based H-bonded network (VATA). (b) Instant and (c) reusable adhesion behavior of VATA relative to cyanoacrylate as an underwater adhesive. Reproduced with permission from ref. [40]. Copyright 2020, American Chemical Society.

Furthermore, indocyanine green (ICG)-labeled TAPE was employed as an effective pH-sensitive probe for gastroesophageal reflux disease (GERD).

In the same year, Lee and coworkers<sup>[37]</sup> developed a biodegradable and water-resistant TA/DNA hybrid hydrogel (TNA) that is prepared by exploiting the hydrogen bonding interactions between the polyphenol of TA and phosphodiester backbone of DNA. Gelation of TNA was attained by mixing TA (pH 1.6) and DNA (pH 7.0) solutions at a stoichiometric ratio of [DNA base pairs]/[TA] = 1.3. However, no gelation was observed upon doubling the stoichiometric value. The tissue adhesiveness of TNA hybrid gel (10.5 ± 0.2 kPa) appeared to be much higher compared with that of native DNA (1.0 ± 1.0 kPa). Critically, the biodegradability and release of encapsulated DNA can be realized from the hydrogels in the physiological medium (pH 7.4) due to the hydrolysis of ester groups of TA. TNA hydrogel showed complete hemostasis within 53 seconds in a bleeding mouse liver, which makes it a useful biomedical hemostatic agent.

After establishing good tissue adhesiveness and hemostatic capabilities, the same group demonstrated the excellent *in vivo* mucoadhesive properties of TAPE, synthesized by a physical blending of PEG-OH and TA.<sup>[37]</sup> Meanwhile, the adhesive force of TAPE was investigated by changing the molar ratio of pyrogallol (TA) to OH groups of PEG that

were found to be significantly enhanced with increasing [TA]/[PEG-OH] ratios (10:1 = 1.7 ± 0.8 kPa; 20:1 = 3.1 ± 0.7 kPa; 30:1 = 25.9 ± 1.5 kPa). After oral feeding the mice, fluorescence imaging tracked the ICG-labeled TAPE. The tape remained on the esophageal mucus layer for several hours before moving to the stomach. Notably, the synthesized TAPE binds strongly to the mucin layer in neutral conditions, whereas it adheres weakly under an acidic milieu.

A major challenge in adhesive research is the reusability of underwater adhesives. The use of well-known cyanoacrylate or epoxy-based adhesives for wet adhesion holds several limitations such as rapid solidification, short working time, lack of reusability, and biological toxicity.<sup>[38,39]</sup> Therefore, the fabrication of nontoxic reusable adhesives is highly desired. Poly(vinyl alcohol) (PVA) and TA-based H-bonded network (VATA), a reusable underwater adhesive was constructed by mixing PVA and TA solutions of equal weights in distilled water, yielded as viscous yellow precipitate (Figure 8a).<sup>[40]</sup> VATA can rapidly (within a few seconds) act as a molecular glue to attach two objects of various materials (glass, iron, polystyrene, aluminum, and stainless steel) in underwater conditions (Figure 8b). Tensile and shear tests showed that the underwater adhesion strength of VATA is around 70 kPa, which remained unaltered even after 10 times attachment-detachment cycles (Figure 8c). However,

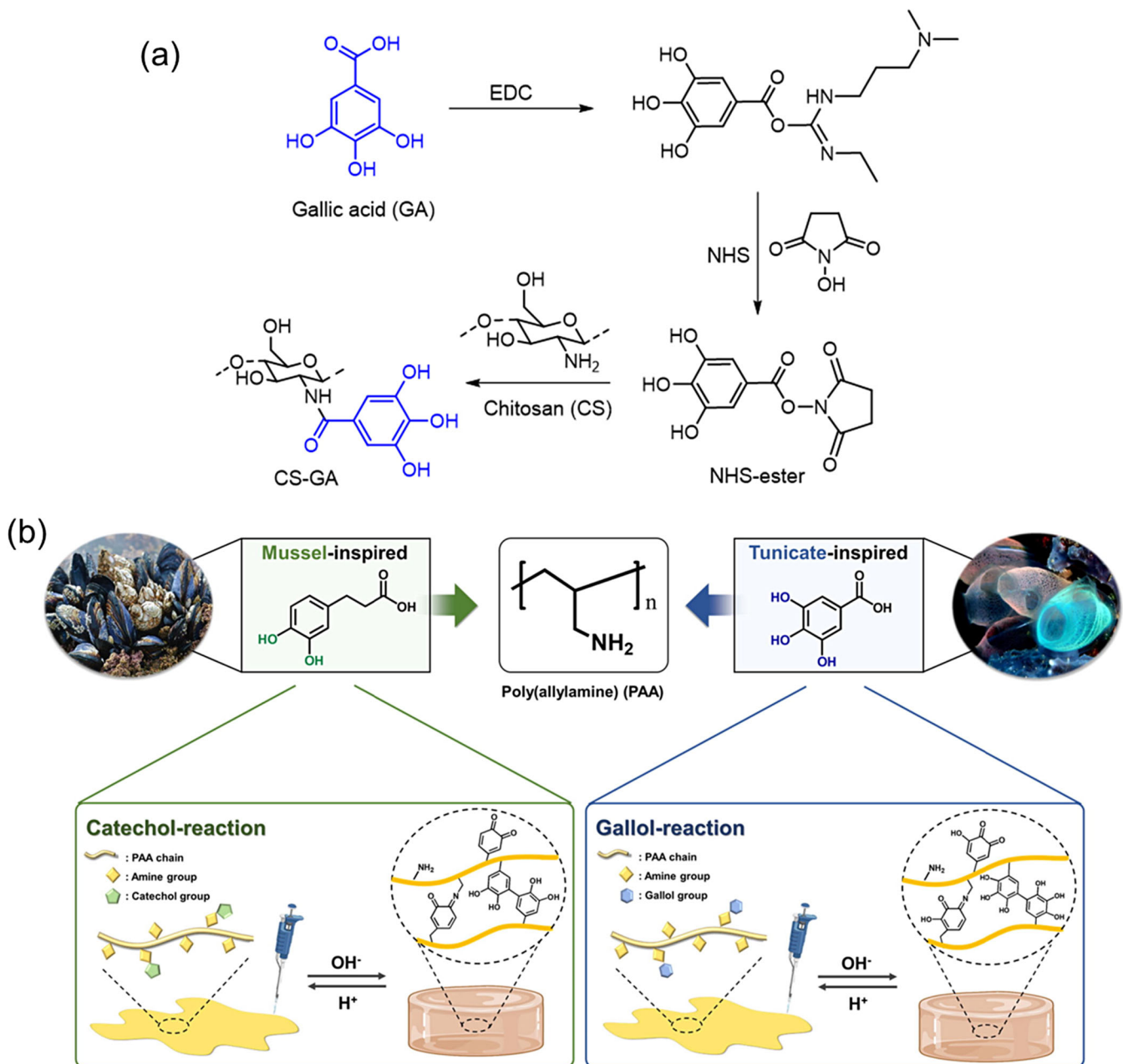


Figure 9. (a) Synthesis of CS-GA conjugates *via* NHS/EDC coupling reaction. (b) Schematic representation of mussel and tunicate-inspired polyallylamine hydrogels. Figure 9a reproduced with permission from ref. [42]. Copyright 2019, Elsevier. Figure 9b reproduced with permission from ref. [16]. Copyright 2021, Elsevier.

cyanoacrylate adhesive exhibits much lower initial tensile adhesion strength (34 kPa) in water, and it immediately loses its adhesiveness after the 2nd cycle. Furthermore, the toxicity of VATA was evaluated using a vertebrate goldfish and an invertebrate nematode (*Caenorhabditis elegans*), suggesting no toxicity for  $\sim 168$  h.

In another work<sup>[41]</sup>, the coexistence of strong adhesion and cohesion was achieved by preparing poly(dimethyl diallyl ammonium chloride) (PDDA)/TA hydrogel (PTFe) using  $\text{FeCl}_3$  as a metal crosslinker. The highest adhesive strength of the hydrogel for polymethyl methacrylate (PMMA), porcine skin and stainless steel are  $75.6 \pm 4.0$ ,  $44.8 \pm 4.0$ , and  $82.1 \pm 4.7$  kPa, respectively. PTFe also showed high mechanical strength (cohesion;  $\sim 0.15$  MPa), rapid self-healing ability and good ionic conductivity ( $\sim 4.3 \text{ S m}^{-1}$ ).

### 2.3. Gallo-rich hydrogels and gallo-containing supramolecular composites

Inspired by non-covalent interactions with proteins, pyrogallols are often modified with polysaccharides (e.g. chitosan and hyaluronic acid (HA)) to achieve gallo-rich hydrogels and/or supramolecular composites with splendid adhesion performance. For example, Hwang and coworkers have developed GA-functionalized chitosan (CS)-based hydrogels using NHS/EDC chemistry (Figure 9a).<sup>[42]</sup> The GA was first activated with NHS-ester, followed by coupling with the amino groups of CS, resulting in CS-GA hydrogels. The hydrogels were further crosslinked separately *via*  $\text{NaIO}_4$  and  $\text{Fe}^{3+}$ -promoted crosslinking. As an *in vitro* wet adhesion test suggests, CS-GA hydrogels exhibit a much higher

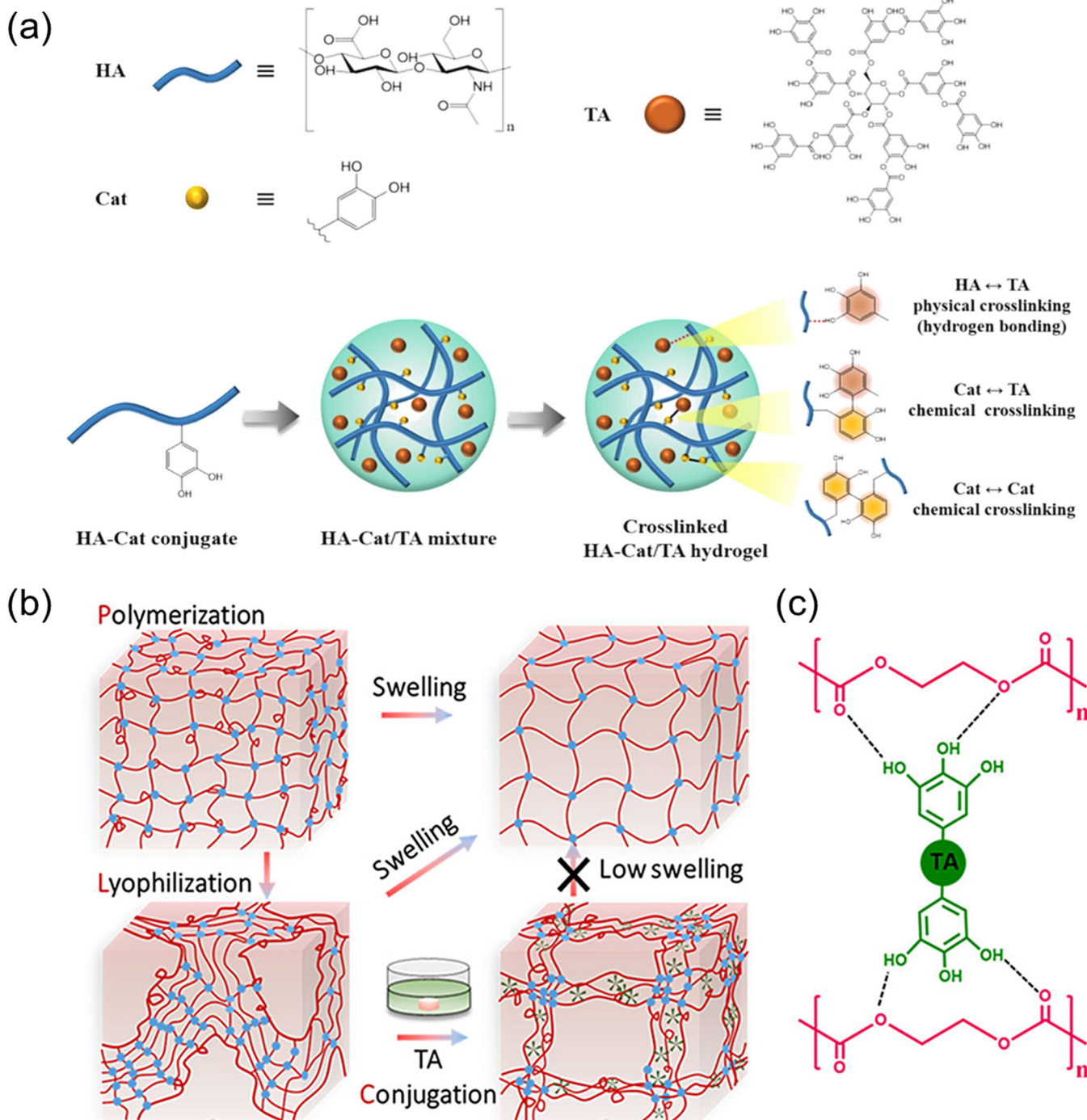


**Figure 10.** (a) Schematic illustration of different interactions in HA-Cat/TA hydrogels. (b) Demonstration of polymerization-lyophilization-conjugation method for the construction of all-in-one PEGDA/TA hydrogels. (c) Representation of the existent H-bonding network in PEGDA/TA hydrogels. Figure a reproduced with permission from ref. [45]. Copyright 2021, Elsevier. Figure b and c adapted with permission from ref. [46]. Copyright 2021, American Chemical Society.

adhesion force on porcine skin ( $\sim 47$  kPa) than commercially available surgical glue, fibrin glue ( $\sim 22.59$  kPa). This is due to the presence of excess hydroxyl and amine groups in the hydrogels that can participate in electrostatic interactions and H-bonding with the biological interfaces. In addition, the hydrogel showed better hemostatic ability compared to gauze and the nascent CS film.

A tunicate-inspired hydrogel was constructed by Liu et. al. using a straightforward yet simple method.<sup>[43]</sup> The hydrogel (GelTHB-Fe) was prepared by mixing gelatin- $\text{FeCl}_3$  with 2,3,4-trihydroxybenzaldehyde (THB). Gelatin was

conjugated with THB *via* Schiff base reaction, and then the precursor turned into a gel in addition of  $\text{Fe}^{3+}$  owing to the formation of hexavalent iron complexes. The resulting hydrogel not only exhibited good adhesive strength but also displayed rapid self-healing, caused by dynamic imine bonds. The average adhesive strengths of GelTHB-Fe to porcine skin, steel, ceramic, and PMMA are 56.5, 147.3, 153.7, and 136.7 kPa, respectively. Additionally, it was shown to simultaneously reduce infection and facilitate wound healing in a diabetic rat model. Similarly, two different polyallyl-amine-based hydrogels were prepared by integrating

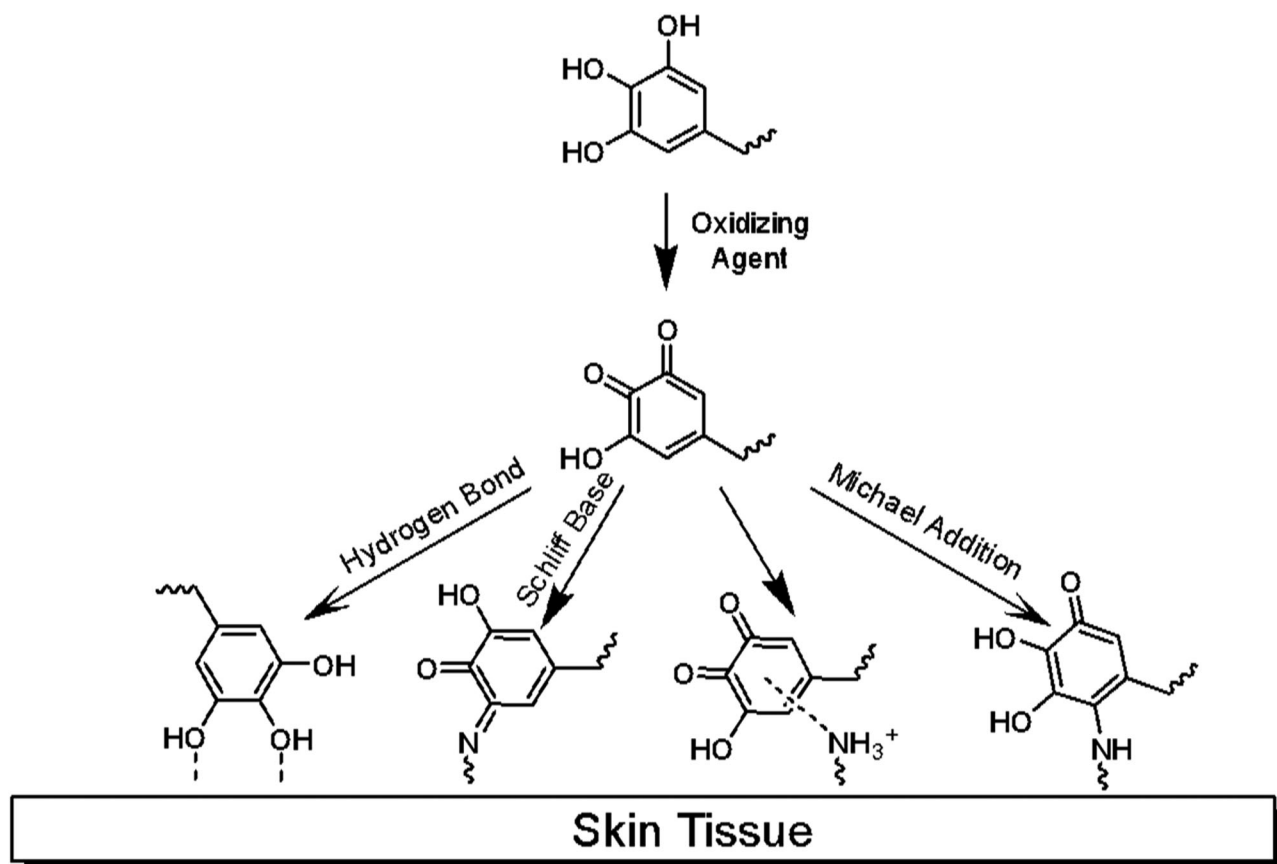


Figure 11. Skin adhesion mechanisms of gallo moiety on polymers.

catechol (PAA-CA) and gallo (PAA-GA) functionalities using Schiff base reaction (pH 7.0) to mimic the wet adhesion properties of mussels and tunics (Figure 9b). Self-cross linkable PAA-CA and PAA-GA hydrogels showed better adhesiveness in wet environments rather than dry environments, due to the synergistic effect of gallo, catechol and amino groups of PAA. In comparison to PAA-CA, PAA-GA hydrogels have shown better adhesion strength, self-healing ability and antibacterial properties.<sup>[16]</sup> Supremacy of such GA-based hydrogels has also been proved by Oommen and coworkers<sup>[44]</sup> where they have evaluated the relative tissue adhesive behavior of HA-GA and HA-DA (dopamine) scaffolds through a rheometric track-adhesion test. The hydrogels were synthesized by carbodiimide coupling between HA and CA/GA using NHS/EDC chemistry. In another report, the adhesive properties of HA-CA conjugates were further improved by the addition of TA (10 pyrogallol per TA) during the fabrication of the gel (HA-Cat/TA).<sup>[45]</sup> This fact attributed to the emergence of additional H-bonding between HA $\leftrightarrow$ TA, chemical crosslinking between Cat $\leftrightarrow$ TA and Cat $\leftrightarrow$ Cat (Figure 10a). The HA-Cat/TA hydrogels were prepared by the co-addition of TA and NaIO<sub>4</sub> as an oxidative crosslinker into an aqueous solution of HA. These hydrogels furnished excellent adhesion on various surfaces, including rubber, glass, aluminum, steel, etc. Notably, the adhesion strength can be altered by varying molar ratios of TA and crosslinker NaIO<sub>4</sub> and the highest value ( $\sim$ 10 kPa; on porcine skin) was obtained with a ratio of Cat: NaIO<sub>4</sub>: TA = 1:2:1.

Wang's research group meticulously developed an all-in-one TA-containing multifunctional hydrogel (PEGDA/TA) adhesives with strong and instant underwater adhesion, high toughness, notch sensitivity, on-demand detachment, low swelling index, self-healability, and tailorabile topography.<sup>[46]</sup> The synthetic strategy involves the utilization of polymerization-lyophilization-conjugation method, in which pyrogallol TA moieties was introduced into the high molecular weight polyethylene glycol diacrylate (PEGDA) covalent network (Figure 10b). Briefly, PEGDA hydrogels were lyophilized to get a porous scaffold, followed by incubation in TA aqueous solutions of different concentrations (10–50 w/v%), leading to a web-like H-bonding network (Figure 10c). PEGDA/TA hydrogels showed strong underwater adhesiveness to porcine skin with a tensile pull-off strength of  $87.9 \pm 9.5$  kPa and  $128.6 \pm 12.4$  kPa for gels consisting of 10% and 50% TA, respectively. These values are way higher than those of commercial adhesives fibrin glue ( $7.4 \pm 0.9$  kPa) and cyanoacrylate ( $17.6 \pm 2.1$  kPa).

Most recently, a new strategy to prepare pyrogallol-based hydrogels by introducing soybean protein isolate (SPI) into the gel network has been developed. SPI, a plant-derived protein, has attracted much attention owing to its widespread distribution, abundant active functions, and good environmental protection.<sup>[47]</sup> It contains numerous  $-\text{OH}$ ,  $-\text{NH}_2$  and  $-\text{COOH}$ , which act as an active site for H-bonds, and concurrently enable the interaction with various substrate surfaces.<sup>[48,49]</sup> SPI-tethered polyacrylamide-pyrogallol/borax hydrogels were prepared by mixing pyrogallol and

**Table 1.** Adhesion properties and applications of gallo containing adhesives polymers.

Polymers	Adhesion strength	Test conditions	Materials for adhesion tests	Applications	References
PEG-TA HMSG	6.2 MPa	Humidified	Glass	Hot melt super glue	[52]
PEG-PPG-PEG, F68	1.1 MPa	In water	Porcine skin tissue	Biomedical adhesive	[59]
TAPVA	200 kPa	In water	Fe-al alloy substrates	Underwater coating adhesive	[53]
TAPE	180 kPa	Dry	Porcine skin tissue	Biomedical adhesive	[29]
PTFe	104.6 kPa	Dry	Porcine skin tissue	Adhesive hydrogel	[35]
VATA	70 kPa	In water	Glass cylinders	Underwater adhesive	[40]
CS-GA	53 kPa	Dry	Porcine skin tissue	Tissue adhesive	[42]

borax in water, followed by the subsequent addition of acrylamide and ammonium persulphate (APS) as polymerizable monomer and initiator. These hydrogels comprised a sufficient number of free pyrogallol groups into the H-bonded as the unwanted autoxidation of gallo was suppressed through borax-promoted chelation. Therefore, polyacrylamide-pyrogallol/borax provided good adhesiveness in both hydrophobic and hydrophilic surfaces with an average adhesion force of  $29.0 \pm 2.0$ ,  $42.7 \pm 2.52$ ,  $68.0 \pm 3.0$ ,  $34.3 \pm 2.51$  kPa on glass, steel, wood, and porcine skin, respectively. The highest adhesion strength on wood surface is most likely due to the synergistic effect of H-bonding,  $\pi-\pi$  stacking, and hydrophobic interactions between the hydrogels and diverse functional groups: COOH, OH, NH<sub>2</sub> on the wood surface. Moreover, polyacrylamide-pyrogallol/borax showed good antibacterial activity against *Escherichia coli* and *Staphylococcus aureus* as they are made of antibacterial pyrogallol and borax.<sup>[50]</sup> Li and Shi *et al.*<sup>[51]</sup> also synthesized antibacterial SPI-based adhesives by co-deposition of catechol and gallo-functionalized polyamines onto the surface of aramid fiber. As disclosed by wet shear strength measurement, the adhesion strength of the hydrogel (1.68 MPa) boosted up to 133.3% to that of the pure SPI adhesives (0.72 MPa). It was believed that the enhanced adhesive behavior of the hydrogel arose from the synergistic interfacial interaction *via* both covalent and hydrogen bonding.

Based on the intrinsic H-bonding feature of GA molecules, the research group of Cui created a new class of supramolecular network between TA and PEG, referred to as hot melt super glue. Various substrate surfaces, namely glass, steel, PMMA, wood can be glued using hot melt super glue. The adhesion strength of hot melt super glue can be tuned from kPa level to 8.8 MPa by varying the repeating units of PEG and TA content. Interestingly, almost no variation in the adhesive strength was found after 8 repetitive attach-detach cycles *via* the heating-cooling process, due to the presence of flexible PEG chains. The advantages of solvent-free hot melt super glue lie in excellent, rapid and repeatable adhesion as well as scalability of synthesis and strong adhesion at low temperature (-196 °C).<sup>[52]</sup>

### 3. Applications

#### 3.1. Tissue adhesives

Tissue adhesives are a subclass of polymers that have gained great attention in the healthcare field due to the ability of tissue adhesives to replace sutures or staples as an alternative method of closing wounds. However, tissue adhesives are

difficult to manufacture, as they need to be able to maintain adhesion in aqueous environments due to the presence of bodily fluids such as sweat and blood, however, most bonds that comprise modern adhesives are very vulnerable to external factors present such as salt and moisture.<sup>[53,54]</sup> While some modern biomedical adhesives exist currently, such as those based on cyanoacrylates, these are not very safe to human cells, and as such can only be used externally on the skin.<sup>[55]</sup> Other biomedical adhesives exist currently such as fibrin glues, however, these fibrin glues have been found to be quite weak in underwater environments, particularly over long periods of time.<sup>[56]</sup> To overcome these disadvantages, gallo-based polymers are able to adhere well to the skin through four different methods shown in Figure 11 attributing to their high tissue adhesion, or the ability to adhere to two surfaces, one of which being biological in nature.<sup>[57]</sup> The basic gallo's adhesion mechanism resembles catechol containing adhesives' which are reviewed elsewhere.<sup>[58]</sup> An overview of the adhesion strengths of polymers discussed throughout this review can be found in Table 1.

The first type of gallo containing tissue adhesive was reported by Kim *et al.* This tissue adhesive is a blending of tannic acid and PEG as shown in Figure 12a.<sup>[29]</sup> The mixture was dissolved in water to create a highly viscous adhesive. This tissue adhesive requires no covalent forming synthetic procedures, allowing large production in a simple procedure. The resulting adhesive, referred to as TAPE, was tested with several differing end groups; however, the highest adhesion strength was from the PEG-amine. The resulting adhesion strength was approximately 0.18 MPa, which is over twice the strength of the commonly used alternatives, such as fibrin glue (0.07 MPa). Kim *et al* also utilized this new biomedical adhesive in a unique method, taking advantage of the large number of ester bonds in tannic acid, as well as the adhesiveness of the new TAPE adhesive. TAPE-OH was utilized as a method for detecting GERD (gastroesophageal reflux disease), by applying the TAPE to the esophagus of a mouse through oral injection. This allows it to then adhere to the tissue along the esophageal tract. GERD is characterized by the high pH in the esophagus. Due to the abundant ester bonds in the tannic acid, if GERD was present in the mouse, the adhesive would degrade by cleaving these ester bonds, which could be detected using fluorescence.

A different approach was utilized by Lee *et al* in which hyaluronic acid was used with gallo moieties as demonstrated in Figure 12b.<sup>[60]</sup> A commercial hyaluronic acid was conjugated with a gallo moiety to the backbone of the commercial hyaluronic acid. This tissue adhesive was employed

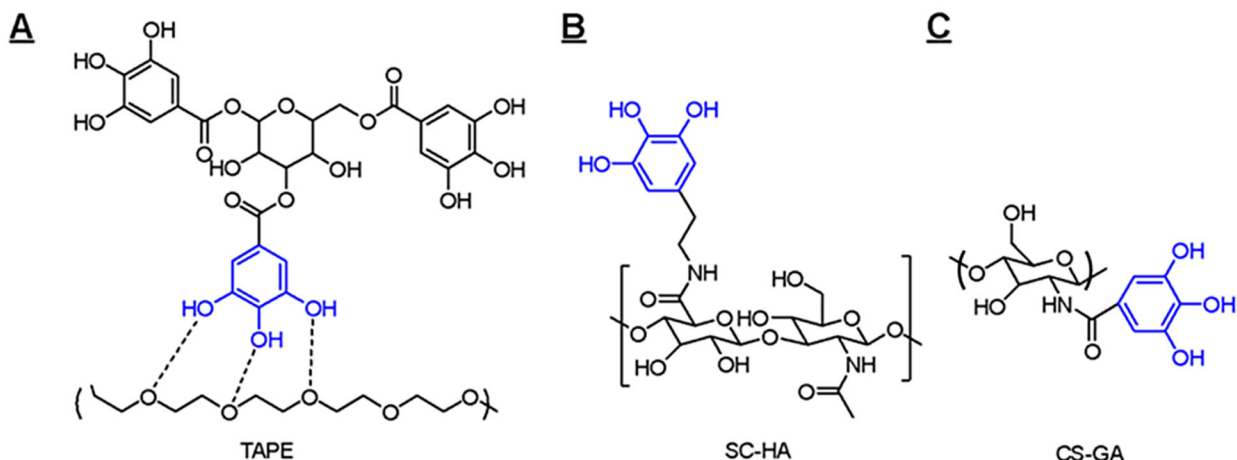


**Figure 12.** Chemical structures of tissue adhesives prepared by the blending of tannic acid and poly(ethylene glycol), hyaluronic acid, and chitosan respectively; a) TAPE<sup>[29]</sup> B) SC-HA<sup>[60]</sup> and C) CS-GA<sup>[42]</sup>, gallol groups in each structure are shown in blue.

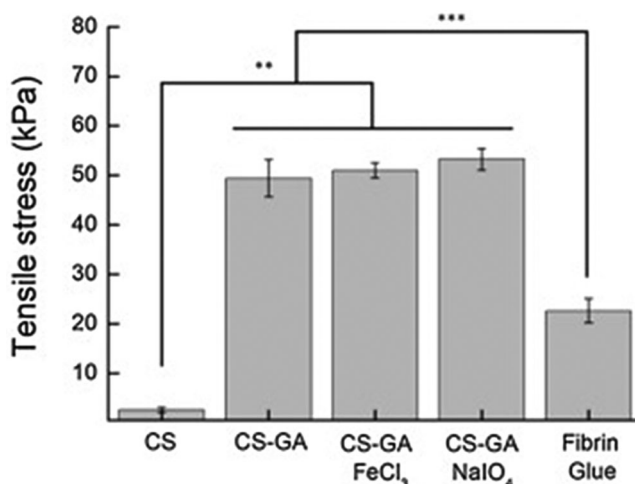


**Figure 13.** Comparison of underwater adhesion strength of pure chitosan, chitosan-gallol gel with and without the addition of iron chloride ( $\text{FeCl}_3$ ) or sodium periodate ( $\text{NaIO}_4$ ), and fibrin glue from Sanandiya *et al.* Polymer chemical structure of CS-GA is shown in Figure 12. CS is chitosan. Reproduced with permission from ref. [42]. Copyright 2018, Elsevier.

as a method of volume augmentation, to correct any sort of volumetric deformity of the skin such as wrinkles. In this report, gallol was utilized primarily for two separate reasons: (1) the ability to self-crosslink, allowing the hyaluronic acid to self-crosslink, and (2) the non-crosslinked gallol groups allowing for greatly improved tissue adhesion in comparison to lone hyaluronic acid. The increased adhesion by the addition of gallol is due to the ability of gallol to react with other gallol groups when it is oxidized. When gallol is oxidized, it will then react with itself, and produce  $\text{H}_2\text{O}_2$ , which will increase the amount of crosslinking that occurs. This allows the hydrogel to highly crosslink on its own without any additional crosslinkers or catalysts needed. The oxidation is biocompatible, allowing it to be done within the injection site to allow very easy delivery, followed by crosslinking of the hydrogel.

Cell viability in this study was tested both following one day of introduction to human dermal fibroblasts, as well as a week following to prove the cell viability of this reaction was completely biocompatible, and the cells remained above

95% viability following a week. This meant that if there is any impact of excel hydrogen peroxide from this reaction in the skin, it does not have a major impact on safety. In addition, the adhesion strength of the self crosslinkable hyaluronic acid was compared to that of chemically crosslinked hyaluronic acid, in which the shear strength was greater than five times when it was self-crosslinked with gallol groups. This can be attributed to the hydrogen bonding of the available hydroxyl groups located throughout the cross-linked gallols, and the metal and ion binding that gallol groups are capable of participating in.

Sanandiya *et al.* also developed a gallol containing adhesive to function as a sealant and hemostatic hydrogel.<sup>[42]</sup> To accomplish this, gallic acid based on sea animal tunics were utilized in conjunction with chitosan to create an adhesive hydrogel shown in Figure 12c with the adhesion from the gallol groups, as well as the biocompatibility and hemostatic capabilities of chitosan. Chitosan has poor solubility at physiological pH values; however, the addition of gallol groups greatly improves the solubility within this pH range. In addition, gallic acid also provides many other properties such as antimicrobial and anti-inflammatory properties. The adhesion of the chitosan-gallol hydrogel (CS-GA) was found to be 47 kPa in 0.1 M PBS, nearly double that of fibrin glue in comparison with around 22.59 kPa. The three hydroxyl groups in gallol, as well as the additional amine groups present in chitosan all contributed to additional adhesion, and the gallol group allowed the adhesion to remain while in aqueous environments. In addition, if the tissue adhesive were to be cured using  $\text{FeCl}_3$  and  $\text{NaIO}_4$  CS-GA had increased adhesion strengths of 51 and 53 kPa respectively, as shown in Figure 13. While the hemostatic capability of chitosan has been reported previously due to the interactions between amines positive charge interacting with the negative charges of platelets, Sanandiya *et al.* quantitatively proved the hemostatic ability utilizing the *in vitro* blood-clotting index (BCI), in which higher numbers are related to better hemostatic capabilities. Gauze and chitosan have BCIs of 92.56% and 95.27%, respectively, while CS-GA has a BCI of  $82.19\% \pm 1.19$ , suggesting that gallol had an impact on

## Esophagus (pH 7.0)

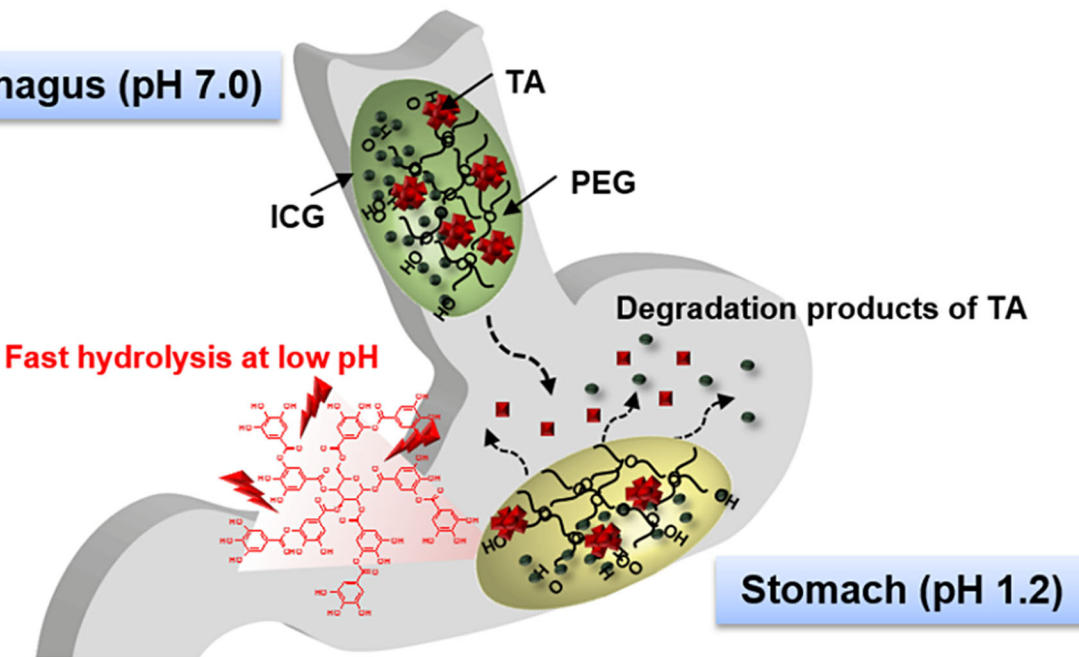


**Figure 14.** Visualization of the process of TAPE degrading within the stomach from the esophageal tract into biocompatible monomers, losing adhesion and releasing the ICG in the process. Reproduced with permission from ref. [37]. Copyright 2016, American Chemical Society.

improving the hemostatic capability of chitosan to be significantly better than that of commercially available gauze.

### 3.2. Drug delivery

One of the major difficulties with efficient drug delivery systems (DDS) is the short residence time at the site of absorption.<sup>[61]</sup> Due to this, biomedical adhesive DDS have been under heavy investigation as a method of delivering drugs to a targeted location for long periods of time through controlled release mechanisms such as diffusion and release through degradation of polymers encapsulating drugs. The previously discussed TAPE biomedical adhesive utilizing tannic acid and PEG was found to also be very valuable as a DDS for esophageal drug delivery for GERD.<sup>[37]</sup> TAPE tissue adhesive was loaded with indocyanine green (ICG), a fluorescent dye that was used as a method of tracking drug delivery *in vivo*. Ideally, any sort of drug that would be used would have a similar diffusion as that of ICG, allowing the researchers to use this tracking method reliably to track DDS speed and delivery path using the method shown in Figure 14. Here, the tannic acid/PEG mixture was loaded with ICG particles and were placed into the esophageal tract. As the polymer degrades in the presence of the high pH present in GERD patients, the degraded products would end up in the stomach where they would be dissolved. The adhesive was first tested *in vitro* to see the degradation, and at a pH of 1.2 (normal for that of individuals with GERD), and a biological pH of 7 as a control, it was found that the rate of degradation was about twice the speed at the higher pH. In the *in vivo* studies, TAPE was compared to both PEG and TA alone, as well as glycerin. The results indicate that the mucoadhesion after 8 h is much more favorable in the TAPE, having nearly

no movement from the application site, while the others moved greatly throughout the esophageal tract. These results suggest that if TAPE were to be applied to a targeted location loaded with some drug, it would then be released at a controllable rate from the degradation and remain on the site of implantation after long periods of time due to the strong adhesion from the gallo groups.

A different approach to drug delivery was utilized by Cho *et al.* utilizing the covalent bonding of pyrogallol (PG) with hyaluronic acid (HA) for tissue sealant and drug delivery such as growth factor, VEGF.<sup>[62]</sup> Gallo groups were under great interest for this functional group largely due to the underwater adhesion, as well as the ability to self-repair through self-crosslinking. This new adhesive named HA-PG was used on various organ tissues such as heart, kidney, and liver from mice to test the ability to not only adhere to skin tissue, but to deliver drugs to the wound site to help with tissue repair. Due to the importance of preventing the wound from opening, any tears within the adhesive can possibly lead to a reopening of the organ wound, which could be extremely detrimental to the intended patient's health. To prevent this, Cho *et al.* use gallo group's ability to crosslink to themselves, to increase the strength over time in the presence of things such as pH changes or oxidation. In addition, the new polymer HA-PG showed no cell cytotoxicity in the presence of human adipose-derived stem cells both *in vitro* as well as *in vivo*, both from the crosslinking of pH changes (using NaOH), or oxidation changes (using NaIO<sub>4</sub>). Testing was also done on mice following the use of the HA-PG loaded with VEGF following hindlimb ischemia. As shown in Figure 15, the hindlimb did not heal well in nearly all cases, particularly with no treatment (PBS). However, while there is some healing from the addition of either the

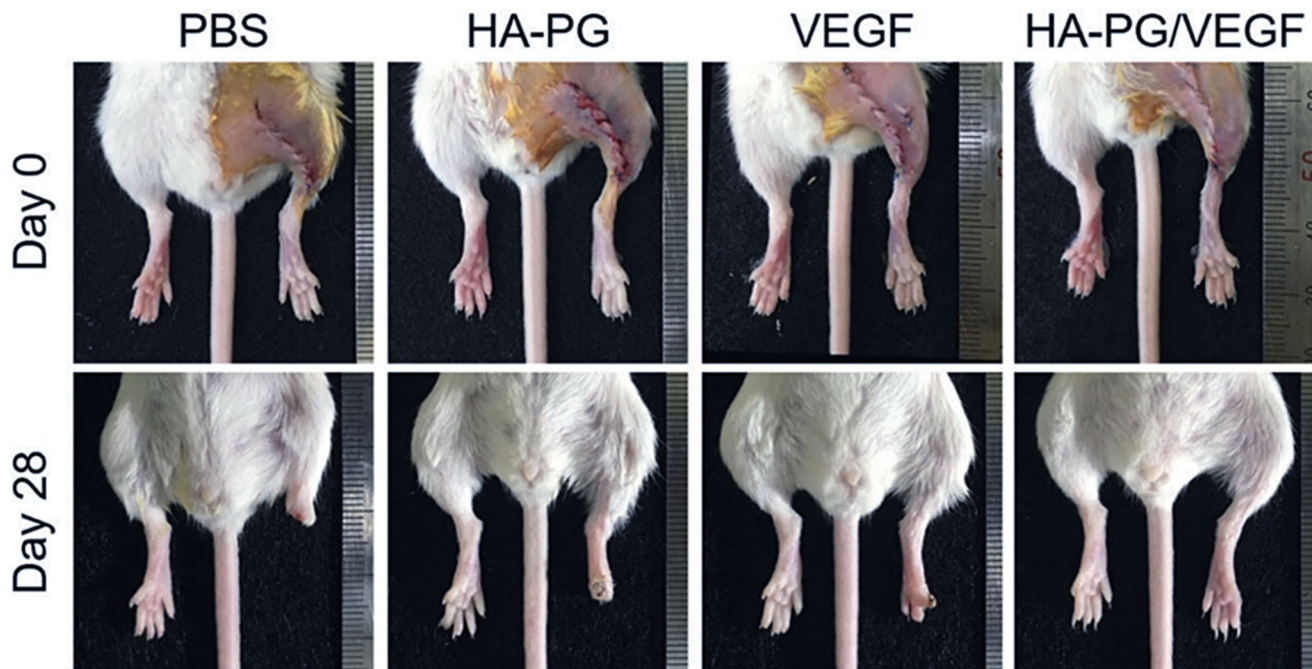


**Figure 15.** Effect of tissue adhesive and growth factor on mice hindleg ischemia done by Cho *et al.* indicating that while the addition of vascular endothelial growth factor (VEGF) heals the wound tremendously, utilizing the covalently bonded hyaluronic acid/pyrogallol (HA-PG) tissue adhesive with VEGF has a greater healing effect than each part individually. Reproduced with permission from ref. [62]. Copyright 2017, Advanced Functional Materials.

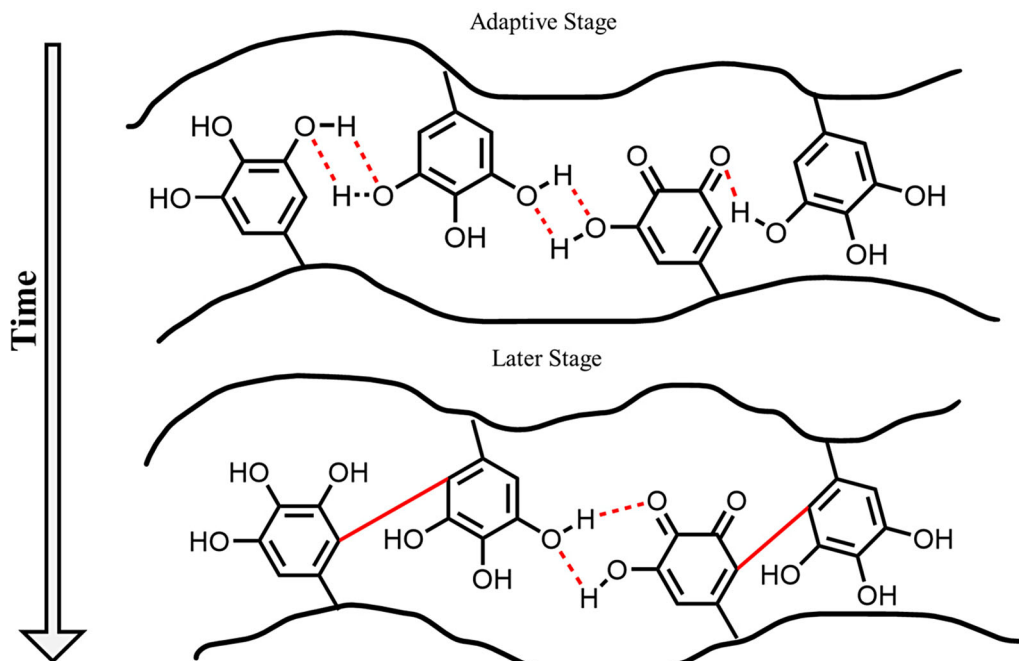


**Figure 16.** The adaptive binder demonstrates structural changes over time changing from hydrogen bonding (dashed red lines) to chemical crosslinking (solid red lines) due to oxidation, leading to the increase of the binder's strength, therefore increasing the number of cycles possible for the lithium-ion batteries. The thick solid black lines can be hyaluronic acid, alginate, or carboxy methyl cellulose.<sup>[63]</sup>

adhesive or the growth factor, combining the two at the mice wound site led to a nearly full recovery in 28 days, confirmed through H&E staining.

### 3.3. Battery and electronics applications

Gallol groups have also gained attention as a method of improving modern electronics, both as binders for lithium-

ion batteries (LIBs) as well as ion conductive gels for biomonitoring. Lee *et al.* report the concept of using gallol groups to facilitate the creation of an “adaptive binder” as a method to overcome difficulties associated with using silicon as an anode material in lithium-ion batteries.<sup>[63]</sup> While silicon as an anode material for lithium-ion batteries has a very high theoretical specific capacity (4200 mAh g<sup>-1</sup> at 45 °C), it suffers from a large amount of expansion and shrinkage as the battery is charged and discharged over the battery’s lifespan.

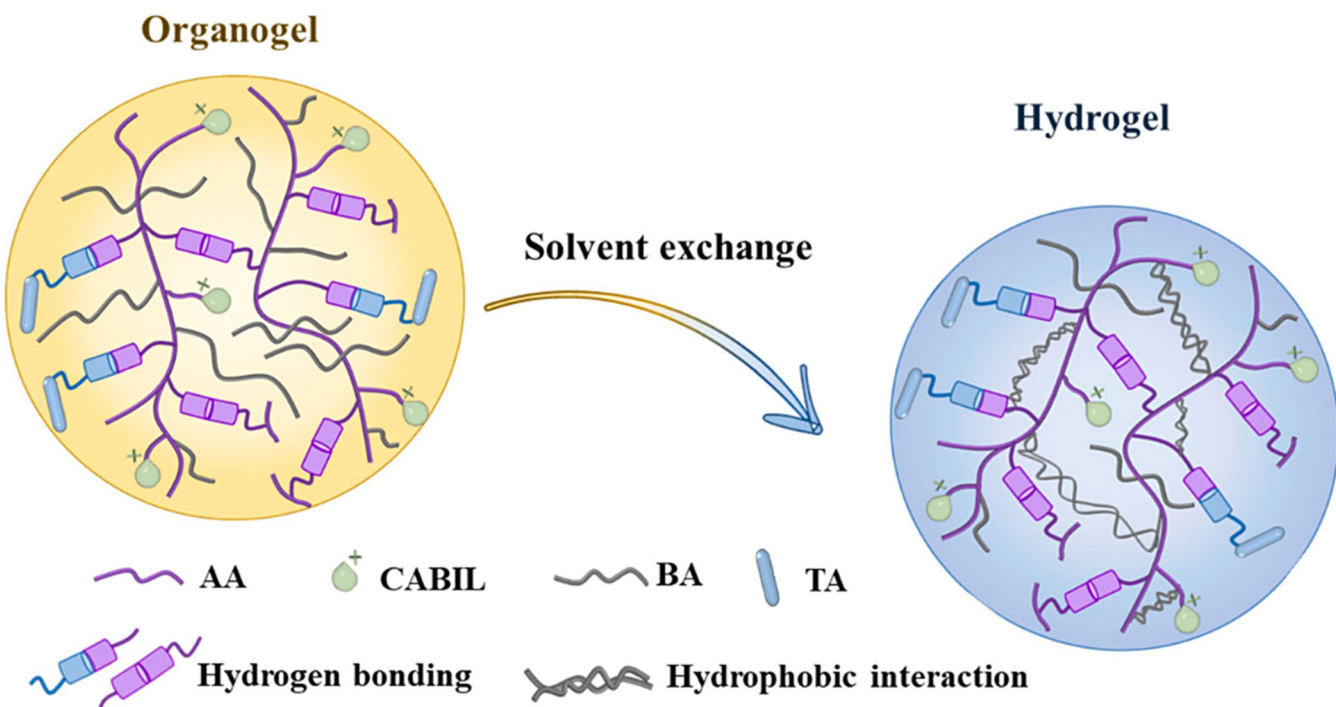


**Figure 17.** Structure of BACT hydrogel utilizing acrylic acid, choline acrylate, butyl acrylate, and tannic acid. While the gel is initially an organogel in DMSO, when the gel is submerged in water, the exchange of solvents results in hydrophobic interaction resulting in the change to a hydrogel. This gel has strong adhesion as well as biocompatibility and ion conductivity. Reproduced with permission from ref. [55]. Copyright 2022, Elsevier.

The major benefit of using gallops as a binder for silicon nanoparticle anodes is due to the ability for gallops to cross-link as they become oxidized over time. During the early stages of a battery's lifetime, the binder must be adaptable due to the large amount of expansion and reduction of the silicon particles in the anode (Figure 16). However, as mentioned by Lee et al. hydrogen bonds, while adaptable and well suited for these early stages, are very weak and can lead to charge leakage over a large number of charge/discharge cycles.

To overcome this, the gallop group's ability to oxidize and form covalent bonds to replace the flexible hydrogen bonds makes them interesting candidates for a LIB binder as shown in Figure 16. In the early stages of the battery's life cycle, when the battery requires a more flexible binder for the expansion and compression of the silicon particles in the anode, gallop is able to utilize weaker hydrogen bonding to allow for these size changes. However, over time, the silicon nanoparticles no longer compress or decompress to the extent at the beginning of the batter's lifespan, in which the gallop groups will begin to crosslink or form galloquinones through oxidation. These covalently crosslinked gallops and galloquinones are a much stronger binder, allowing less charge to be lost and increasing the number of cycles possible by the LIB. Comparing a hyaluronic acid (HA) binder to another hyaluronic acid binder with gallop addition (HA-GA), it was found that after 100 cycles, the pure HA binder retained only 37.9% of the initial capacity, while HA-GA binder still retained 69.2% of its initial charge with a loading of  $1 \text{ mg cm}^{-2}$ .

Another major concern for electronics is the ability to use bioelectronics in an aqueous environment, such as

underwater due to the poor water resistance and underwater adhesion. To bypass these obstacles, Sun *et al.* developed a new ionic liquid utilizing gallop groups from tannic acid as well as choline-based bioionic liquid.<sup>[55]</sup> This newly developed gel had strong adhesion properties from the tannic acid, as well as biocompatibility and ion conductivity. This ionic gel utilizing butyl acrylate, acrylic acid, choline acrylate, and tannic acid (BACT) (named BACT and shown in Figure 17) was employed with electrocardiography (ECG) and electromyography (EMG) as a method of tracking bio-signals while in an underwater environment such as a diver. Following multiple wet peel adhesion tests of this new BACT gel, it was found that in a large number of solutions ranging from water of pH 5–9, seawater, and PBS, the adhesion does not change in any major way over a period of time. In addition, the adhesion of the BACT gels is applicable to a large number of materials such as swimsuits, skin, and PVC, among others. While similar gel electrodes fail after only a single day, the BACT gel maintains strong underwater adhesion even after 15 days, while still maintaining functionality as an ionic gel. Not only was the ionic gel capable of accurate underwater monitoring EMG, but also can be compared to other commercial gel electrodes for monitoring electroencephalogram (EEG) *in vivo*, in which the signal-to-noise ratio is significantly smaller, about a third of the noise (20 uV compared to 65 uV).

### 3.4. Applications in coating

Due to the external environmental contact to the surface of a material for any application, surface modification is a very important and widely used method to improve the

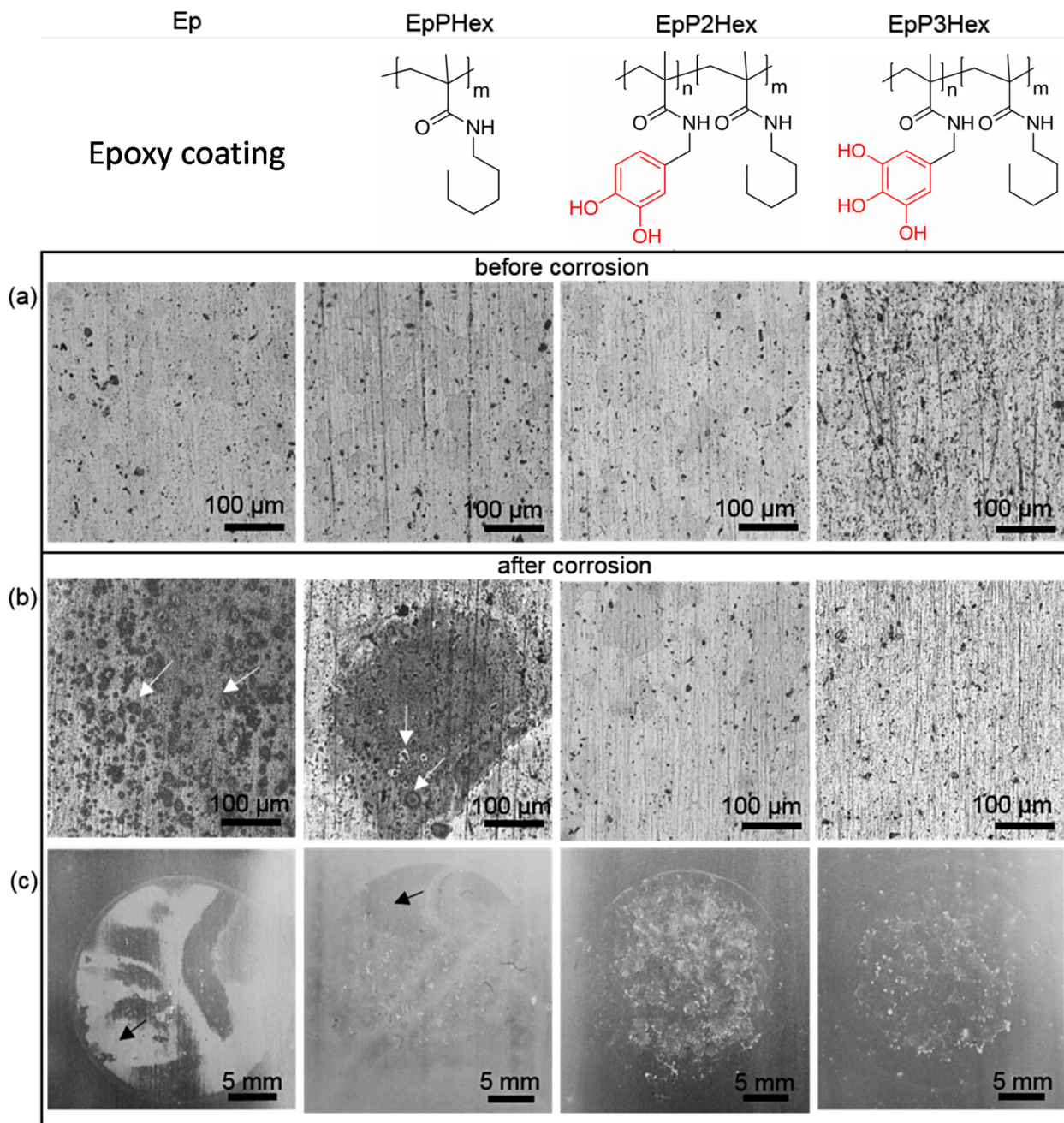


**Figure 18.** Optical images of aluminum substrates with peeled-off coatings before (a) and after (b) 100-day immersion tests, as well as images of aluminum substrates covered with the epoxy coatings (c) after 100-day immersion tests. Arrows point to the pits in the aluminum substrates (b) or the corrosion products under the epoxy coatings (c). Reproduced with permission from ref. [67]. Copyright 2018, American Chemical Society.

functionality of a material.<sup>[64]</sup> One convenient technique of surface modifications is coating. Coating is a method wherein the coating material(s) form a thin layer that non-covalently/covalently adheres to the substrate.<sup>[65]</sup> Gallol containing polymers show strong and effective binding to metallic surface via noncovalent coordination and organic surface with covalent.<sup>[66]</sup> These excellent adhesion properties are applied for surface coating particularly for metallic surface.

Poly(gallol methacrylamide-co-hexyl methacrylamide) was used to protect aluminum alloy surface.<sup>[67]</sup> Aluminum and its alloy has a resistance against oxidation because of the aluminum oxide layer on the surface. However, chloride

ions can still damage the aluminum surface because chloride ions penetrate the aluminum oxide layer followed by corrosion of the aluminum. To prevent such an oxidation, poly(gallol methacrylamide-co-hexyl methacrylamide), which demonstrated excellent antioxidant activity and adhesion on a monolayer on the metal substrate, was developed and comparatively tested with classic coating polymers on aluminum. As shown in Figure 4, aluminum alloy were coated with epoxy polymer (Ep), epoxy polymer + poly(hexyl methacrylamide) (EpPHex), epoxy polymer + poly(catechol methacrylamide-co-hexyl methacrylamide) (EpP2Hex), and epoxy polymer + poly(gallol methacrylamide-co-hexyl methacrylamide) (EpP3Hex). According to the test result with gallol

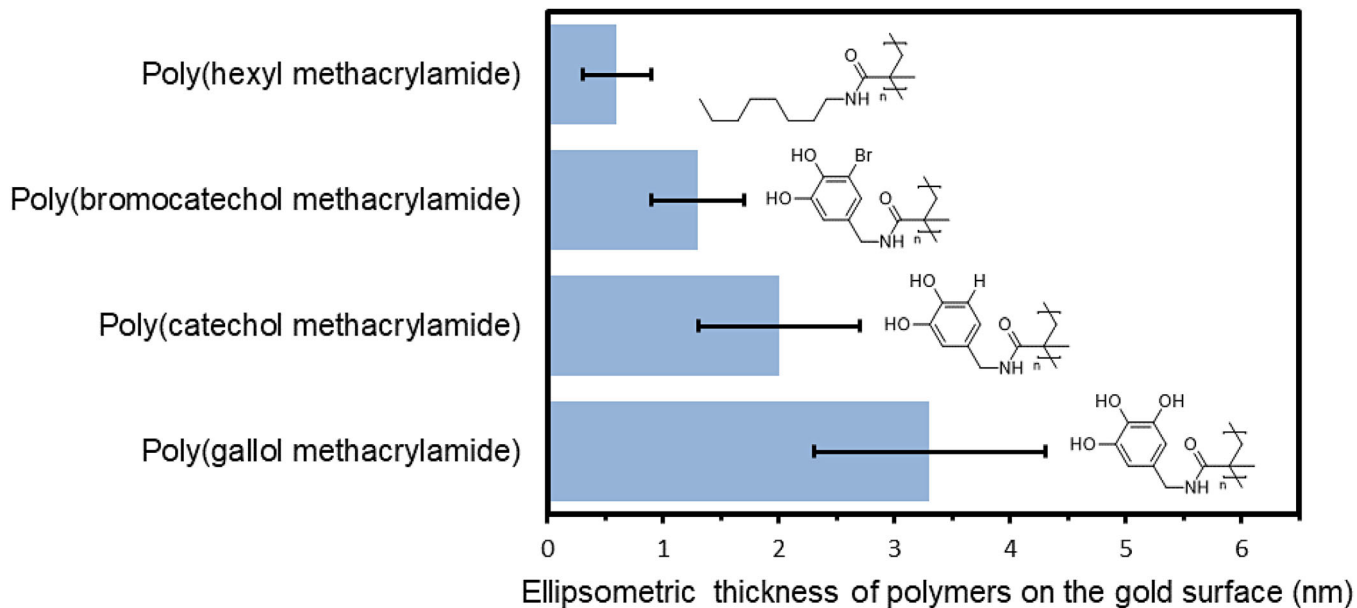


Figure 19. Coating layer thickness of gallol containing polymer and other polymers on gold surface.<sup>[68]</sup>

and catechol containing polymers (EpP2Hex and EpP3Hex), the coating materials did not lose coating after 60 days because of their hydrophobicity and strong bonding to aluminum surface via gallol surface moiety. Furthermore, there was no corrosion observed on the aluminum surface with gallol and catechol containing polymer coating even after 100 days. However, classic epoxy coating and EpPHex showed serious corrosion on the aluminum surface after 100 days (Figure 18).<sup>[67]</sup>

In 2018, poly(gallol methacrylamide) was reported by Hlushko et al.<sup>[68]</sup> for gold surface coating. In this report, four polymers, poly (gallol methacrylamide), poly (catechol methacrylamide), poly (bromo catechol methacrylamide), and poly(hexyl methacrylamide), were studied with various coating thickness. Gallol containing polymer, poly (gallol methacrylamide), formed the thickest monolayer of  $\sim 3.3 \pm 1.0$  nm, catechol containing polymer showed an intermediate thickness of  $2.0 \pm 0.7$  nm, and the bromocatechol containing polymer formed the thinnest layer with  $1.3 \pm 0.4$  nm thickness (Figure 19)<sup>[68]</sup>. This trend can be explained by differences from intramolecular hydrogen bonding strength between the polyphenolic units and gold surface. The gallol containing polymer formed the strongest hydrogen bonds due to the most hydroxyl groups in polymer chains. The catechol containing polymers form weaker hydrogen bonding than gallol group containing polymers due to a smaller number of hydroxyl groups on a single benzene ring (2 vs. 3). Therefore, gallol polymers yields thicker adsorbed layers than catechol's. Poly(hexyl methacrylamide), that does not contain phenol/catechol/gallol groups formed the thinnest coating layer with  $0.6 \pm 0.3$  nm thickness due to lack of hydrogen bonding as shown in Figure 19.

Various nanoparticle coatings with gallol groups were reported in 2013 by Ejima et al. Tannic acid was used as a source of gallol groups. Multiple tannic acids were linked by coordination bonding through Fe(III) in a similar way to polymerization of tannic acids. To make a coating layer,

tannin acid solution and  $\text{FeCl}_3 \cdot 3\text{H}_2\text{O}$  solution sequentially added to the water, then vigorously mixed for a few seconds. As shown in Figure 20, the pH of this solution was gradually raised by adding 1 N NaOH solution to pH 8 to lead to more coordination bonding between gallol and Fe(III). The coordination between Fe(III) and tannic acid is pH-dependent. It leads to a color change of Fe(III)-tannic acid complex suspension. At low pH (below 2), most of hydroxyl groups are protonated, which lead to the formation of mono-complex (colorless suspension) and rapid destabilization of crosslinks. At  $3 < \text{pH} < 6$ , the complex suspension is blue, indicating bis-complex. The disassembly rate of Fe(III)-tannic acid complex at pH 4.0 is much slower than the complex at pH 3.0. Above pH 7.0, most of hydroxyl groups are deprotonated, and therefore, tris-complex is formed with red color. In pH 7.4, 90% of Fe(III)-tannic acid complex still remained intact after 10 days of incubation. The synthesized complexes are coated on various particles such as  $\text{CaCO}_3$ , glasses, golds, polydimethylsiloxane (PDMS), and *E. coli* using a relatively simple method, vigorous mixing for a few seconds under controlled pH (Figure 20).<sup>[14]</sup>

### 3.5 3D Inks for printing

The 3D bioprinting is an important technique in biomedical science and engineering because of its capability of fabricating very sophisticated, tailor-made, cell-laden structures for tissue repair and disease modeling.<sup>[69,70]</sup> Various bioinks which are materials used in 3D bioprinting have been reported for establishing a cell-friendly environment (Figure 21). The basic requirements of a cell suitable bioink are (1) low viscosity for convenient extrusion, and (2) fast curing rate after printing.

Gallol groups containing compounds are suitable for 3D bioprinting because of rapid gelation via hydrogen bonding and oxidative crosslinking. A 3D bioink, mixture of gallol modified hyaluronic acid (HA-Ga) and gallol-gelatin (GEL-

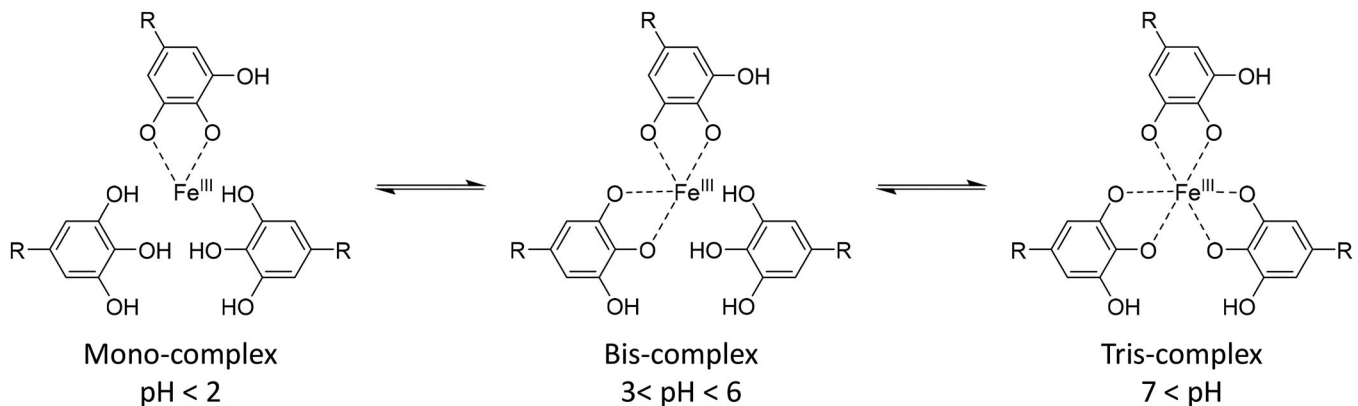


Figure 20. Three pH-dependent transitions of Fe(III)-TA complexes. R represents the remainder of a tannic acid chemical structure.<sup>[14]</sup>

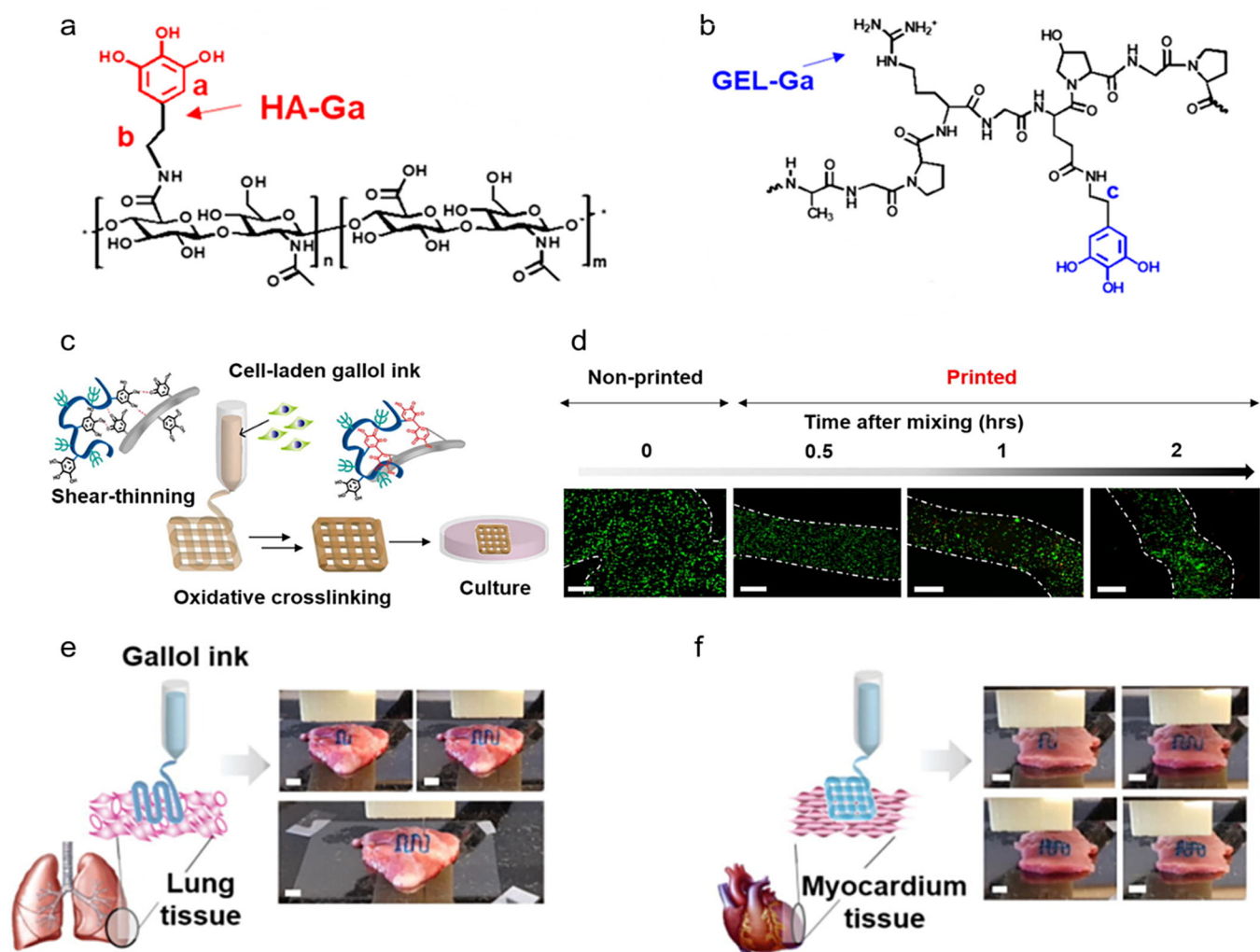
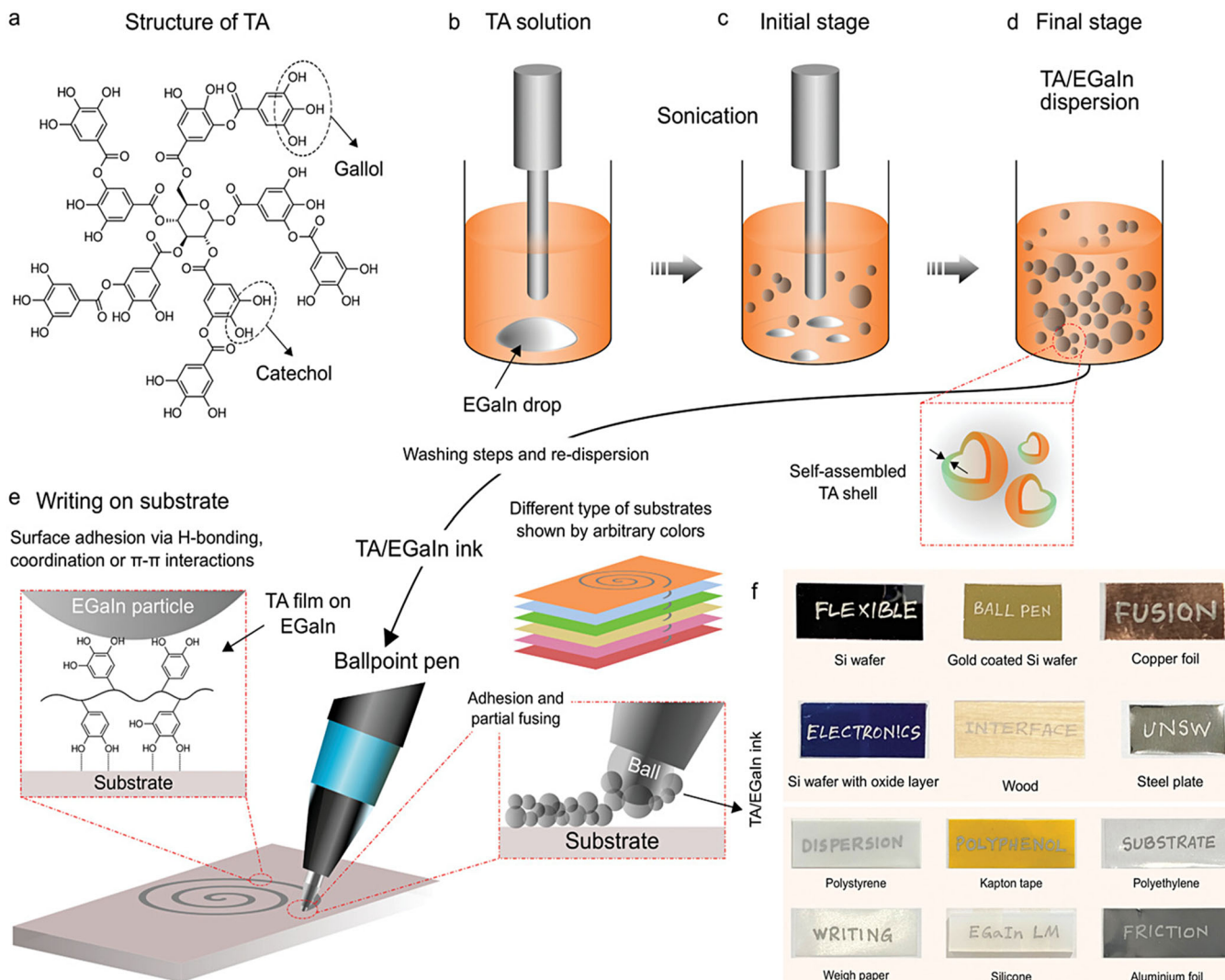


Figure 21. Molecular structure of (a) HA-Ga and (b) GEL-Ga. (c) Schematic description of the 3D printing of cell-laden gallol ECM inks and subsequent cell culture. (d) Fluorescent images. Schematics and images of printing of the gallol ink (containing blue food coloring dye) on (e) porcine lung and (f) myocardium tissues. Scale bars of 4 mm. Reproduced with permission from ref. [71]. Copyright 2019, Elsevier.

Ga), was reported in 2018 by Burdick et al.<sup>[71]</sup> This bioink showed shear-thinning properties during extrusion and fast gelation after extrusion. Also, the bioink allowed covalent crosslinking between each quinone form which is an oxidation form of gallol group over time resulting enhancement on mechanical properties. After the 3D printing process, 95% of loaded cells were still alive. Both cell proliferation

and cell spreading activities were observed at the printed structures. The bioink was directly printable onto live tissues such as lung and heart because of their excellent adhesion properties on soft tissues (Figure 21e and f).

In 2021, self-assembled tannic acid-eutectic gallium-indium alloy particles (TA/EGaIn) are reported for an application in a ball point pen ink (Figure 22).<sup>[72]</sup> Generally, surface patterning



**Figure 22.** Schematic presentation of the ballpoint pen writing process. (a) Structure of tannic acid. (b-d) Schematic of initial to final stages of the preparation of TA/EGaIn ink particles. (e) Schematic of the writing/patterning process using a ballpoint pen filled with the TA/EGaIn inks. (f) Written traces on various flexible substrates. Reproduced with permission from ref. [72]. Copyright 2020, Wiley-VCH.

of liquid metal has several limits including excessively high surface tension and fluidity which cause an unwanted phase separation.<sup>[73]</sup> Another problem is the formation of oxidized layer on the ink during the extrusion. This oxidized layer blocks the patterning nozzle.<sup>[74,75]</sup> To solve these listed issues, tannic acid is used as an effective dispersant of liquid metal, eutectic gallium-indium alloy. Gallo functional group of tannic acid successfully interacted with  $\text{Ga}^{3+}$  ion similarly to  $\text{Fe}^{3+}$  ion to make a self-assembled tannic acid shell on eutectic gallium-indium alloy particles with coordination complex. The self-assembled tannic acid shell (see Figure 22) allowed enhanced dispersion of eutectic gallium-indium alloy particles. The gallo group in tannic acid provides adhesion properties to self-assembled tannic acid-eutectic gallium-indium alloy particles, so that the ink can be written on universal substrates. (Figure 22).<sup>[72]</sup>

#### 4. Conclusions and outlook

In this review, we summarized various synthesis methods and applications of gallo containing adhesive polymers. The

gallo is highly comparative to catechol, which has been studied extensively for various polymer designs and applications. The similarity of chemical structure between gallo and catechol will enable gradual replacement of catechol containing polymers to gallo containing polymers in future research. However, the adhesion mechanism explanations of gallo containing polymers are still relying on the mechanism of catechol groups without comprehensive experimental studies. The oxidation, which impacts adhesion and further reactions, of gallo would behave different from that of catechol. The oxidation reactions, related mechanisms, and following reactions of gallo have not been thoroughly studied. Covalent bond forming reactions from the gallo moiety cannot be the same as catechol due to the distinctive electrostatic natures on the aromatic ring of gallo. Likewise, the understanding of the formation of gallo's covalent bond reaction on polymer will prevent unwanted reactions for adhesive applications as well as creating new applications other than adhesives. The most outstanding deficiency of the present gallo containing adhesive polymers research is a lack of sophisticatedly designed multifunctional polymers.

The multifunctionality of an adhesive is essential for advanced applications such as biomedical adhesives. Unlike lab experiments, actual adhesive application occurs in complex environments such as diverse humidity, temperature, pH, darkness, surface types, and life spans. In this context, there is large room to develop precisely synthesized multi-functional gallo containing adhesive polymers.

## References

[1] Ryu, J. H.; Hong, S.; Lee, H. Bio-Inspired Adhesive Catechol-Conjugated Chitosan for Biomedical Applications: A Mini Review. *Acta Biomater.* **2015**, *27*, 101–115. DOI: [10.1016/j.actbio.2015.08.043](https://doi.org/10.1016/j.actbio.2015.08.043).

[2] Kord Forooshani, P.; Lee, B. P. Recent Approaches in Designing Bioadhesive Materials Inspired by Mussel Adhesive Protein. *J. Polym. Sci. A Polym. Chem.* **2017**, *55*, 9–33. DOI: [10.1002/pola.28368](https://doi.org/10.1002/pola.28368).

[3] Lee, B. P.; Messersmith, P. B.; Israelachvili, J. N.; Waite, J. H. Mussel-Inspired Adhesives and Coatings. *Annu. Rev. Mater. Res.* **2011**, *41*, 99–132. DOI: [10.1146/annurev-matsci-062910-100429](https://doi.org/10.1146/annurev-matsci-062910-100429).

[4] Moulay, S. Dopa/Catechol-Tethered Polymers: Bioadhesives and Biomimetic Adhesive Materials. *Polym. Rev.* **2014**, *54*, 436–513. DOI: [10.1080/15583724.2014.881373](https://doi.org/10.1080/15583724.2014.881373).

[5] Hofman, A. H.; van Hees, I. A.; Yang, J.; Kamperman, M. Bioinspired Underwater Adhesives by Using the Supramolecular Toolbox. *Adv. Mater.* **2018**, *30*, 1704640. DOI: [10.1002/adma.201704640](https://doi.org/10.1002/adma.201704640).

[6] Shin, M.; Lee, H. Gallo-Rich Hyaluronic Acid Hydrogels: Shear-Thinning, Protein Accumulation against Concentration Gradients, and Degradation-Resistant Properties. *Chem. Mater.* **2017**, *29*, 8211–8220. DOI: [10.1021/acs.chemmater.7b02267](https://doi.org/10.1021/acs.chemmater.7b02267).

[7] Shin, M.; Park, E.; Lee, H. Plant-Inspired Pyrogallol-Containing Functional Materials. *Adv. Funct. Mater.* **2019**, *29*, 1903022 (1–26). DOI: [10.1002/adfm.201903022](https://doi.org/10.1002/adfm.201903022).

[8] Ozawa, T.; Lilley, T. H.; Haslam, E. Polyphenol Interactions: Astringency and the Loss of Astringency in Ripening Fruit. *Phytochemistry* **1987**, *26*, 2937–2942. DOI: [10.1016/S0031-9422\(00\)84566-5](https://doi.org/10.1016/S0031-9422(00)84566-5).

[9] Bate-Smith, E. C. Haemanalysis of Tannins: The Concept of Relative Astringency. *Phytochemistry* **1973**, *12*, 907–912. DOI: [10.1016/0031-9422\(73\)80701-0](https://doi.org/10.1016/0031-9422(73)80701-0).

[10] Quideau, S.; Deffieux, D.; Douat-Casassus, C.; Pouységuy, L. Plant Polyphenols: Chemical Properties, Biological Activities, and Synthesis. *Angew. Chem. Int. Ed. Engl.* **2011**, *50*, 586–621. DOI: [10.1002/anie.201000044](https://doi.org/10.1002/anie.201000044).

[11] Shin, M.; Ryu, J. H.; Park, J. P.; Kim, K.; Yang, J. W.; Lee, H. DNA/Tannic Acid Hybrid Gel Exhibiting Biodegradability, Extensibility, Tissue Adhesiveness, and Hemostatic Ability. *Adv. Funct. Mater.* **2015**, *25*, 1270–1278. DOI: [10.1002/adfm.201403992](https://doi.org/10.1002/adfm.201403992).

[12] Chung, J. E.; Tan, S.; Gao, S. J.; Yongyongsoontorn, N.; Kim, S. H.; Lee, J. H.; Choi, H. S.; Yano, H.; Zhuo, L.; Kurisawa, M.; et al. Self-Assembled Micellar Nanocomplexes Comprising Green Tea Catechin Derivatives and Protein Drugs for Cancer Therapy. *Nat. Nanotechnol.* **2014**, *9*, 907–912. DOI: [10.1038/nnano.2014.208](https://doi.org/10.1038/nnano.2014.208).

[13] Liu, B.; Yan, W. Lipophilization of EGCG and Effects on Antioxidant Activities. *Food Chem.* **2019**, *272*, 663–669. DOI: [10.1016/j.foodchem.2018.08.086](https://doi.org/10.1016/j.foodchem.2018.08.086).

[14] Ejima, H.; Richardson, J. J.; Liang, K.; Best, J. P.; van Koeverden, M. P.; Such, G. K.; Cui, J.; Caruso, F. One-Step Assembly of Coordination Complexes for Versatile Film and Particle Engineering. *Science* **2013**, *341*, 154–157. DOI: [10.1126/science.1237265](https://doi.org/10.1126/science.1237265).

[15] Zhan, K.; Kim, C.; Sung, K.; Ejima, H.; Yoshie, N. Tunicate-Inspired Gallo Polymers for Underwater Adhesive: A Comparative Study of Catechol and Gallo. *Biomacromolecules* **2017**, *18*, 2959–2966. DOI: [10.1021/acs.biomac.7b00921](https://doi.org/10.1021/acs.biomac.7b00921).

[16] Lee, S. Y.; Lee, J. N.; Chathuranga, K.; Lee, J. S.; Park, W. H. Tunicate-Inspired Polyallylamine-Based Hydrogels for Wet Adhesion: A Comparative Study of Catechol- and Gallo-Functionalities. *J. Colloid Interface Sci.* **2021**, *601*, 143–155. DOI: [10.1016/j.jcis.2021.05.101](https://doi.org/10.1016/j.jcis.2021.05.101).

[17] Zhan, K.; Ejima, H.; Yoshie, N. Antioxidant and Adsorption Properties of Bioinspired Phenolic Polymers: A Comparative Study of Catechol and Gallo. *ACS Sustain. Chem. Eng.* **2016**, *4*, 3857–3863. DOI: [10.1021/acssuschemeng.6b00626](https://doi.org/10.1021/acssuschemeng.6b00626).

[18] Faure, E.; Falentin-Daudré, C.; Jérôme, C.; Lyskawa, J.; Fournier, D.; Woisel, P.; Detrembleur, C. Catechols as Versatile Platforms in Polymer Chemistry. *Prog. Polym. Sci.* **2013**, *38*, 236–270. DOI: [10.1016/j.progpolymsci.2012.06.004](https://doi.org/10.1016/j.progpolymsci.2012.06.004).

[19] Mishra, A. K.; Hwang, J. H.; Min, J. H.; Park, J.; Lee, E. Metal Scavenging Resin Tethered with Catechol or Gallo Binders via Reversible Addition – Fragmentation Chain Transfer Polymerisation. *Polymer (Guildf)* **2022**, *247*, 124794. DOI: [10.1016/j.polymer.2022.124794](https://doi.org/10.1016/j.polymer.2022.124794).

[20] White, J. D.; Wilker, J. J. Underwater Bonding with Charged Polymer Mimics of Marine Mussel Adhesive Proteins. *Macromolecules* **2011**, *44*, 5085–5088. DOI: [10.1021/ma201044x](https://doi.org/10.1021/ma201044x).

[21] Heo, J.; Kang, T.; Jang, S. G.; Hwang, D. S.; Spruell, J. M.; Killops, K. L.; Waite, J. H.; Hawker, C. J. Improved Performance of Protected Catecholic Polysiloxanes for Bioinspired Wet Adhesion to Surface Oxides. *J. Am. Chem. Soc.* **2012**, *134*, 20139–20145. DOI: [10.1021/ja309044z](https://doi.org/10.1021/ja309044z).

[22] Cheng, B.; Ishihara, K.; Ejima, H. Bio-Inspired Immobilization of Low-Fouling Phospholipid Polymers: Via a Simple Dipping Process: A Comparative Study of Phenol, Catechol and Gallo as Tethering Groups. *Polym. Chem.* **2020**, *11*, 249–253. DOI: [10.1039/C9PY00625G](https://doi.org/10.1039/C9PY00625G).

[23] Bell, G. I. Theoretical Models for the Specific Adhesion of Cells to Cells or to Surfaces. *Adv. Appl. Probab.* **1980**, *12*, 566–567. DOI: [10.1017/S0001867800035254](https://doi.org/10.1017/S0001867800035254).

[24] Vega-Arroyo, M.; Lebreton, P. R.; Rajh, T.; Zapol, P.; Curtiss, L. A. Density Functional Study of the TiO<sub>2</sub>-Dopamine Complex. *Chem. Phys. Lett.* **2005**, *406*, 306–311. DOI: [10.1016/j.cplett.2005.03.029](https://doi.org/10.1016/j.cplett.2005.03.029).

[25] Yu, J.; Cheng, B.; Ejima, H. Effect of Molecular Weight and Polymer Composition on Gallo-Functionalized Underwater Adhesive. *J. Mater. Chem. B* **2020**, *8*, 6798–6801. DOI: [10.1039/d0tb00706d](https://doi.org/10.1039/d0tb00706d).

[26] Liu, F.; Liu, X.; Liu, W.; Gu, H. ROMP Synthesis of Gallo-Containing Polymer Hydrogels for in Situ Fabrication of AuNPs and AgNPs Composites as Recyclable Catalysts for the Degradation of 4-Nitrophenol. *Polymer (Guildf)* **2021**, *219*, 123539. DOI: [10.1016/j.polymer.2021.123539](https://doi.org/10.1016/j.polymer.2021.123539).

[27] Liu, F.; Long, Y.; Zhao, Q.; Liu, X.; Qiu, G.; Zhang, L.; Ling, Q.; Gu, H. Gallo-Containing Homopolymers and Block Copolymers: ROMP Synthesis and Gelation Properties by Metal-Coordination and Oxidation. *Polymer (Guildf)* **2018**, *143*, 212–227. DOI: [10.1016/j.polymer.2018.04.016](https://doi.org/10.1016/j.polymer.2018.04.016).

[28] Hagerman, A. E. Radial Diffusion Method for Determining Tannin in Plant Extracts. *J. Chem. Ecol.* **1987**, *13*, 437–449. DOI: [10.1007/BF01880091](https://doi.org/10.1007/BF01880091).

[29] Kim, K.; Shin, M.; Koh, M. Y.; Ryu, J. H.; Lee, M. S.; Hong, S.; Lee, H. TAPE: A Medical Adhesive Inspired by a Ubiquitous Compound in Plants. *Adv. Funct. Mater.* **2015**, *25*, 2402–2410. DOI: [10.1002/adfm.201500034](https://doi.org/10.1002/adfm.201500034).

[30] Khan, N. S.; Ahmad, A.; Hadi, S. M. Anti-Oxidant, pro-Oxidant Properties of Tannic Acid and Its Binding to DNA. *Chem. Biol. Interact.* **2000**, *125*, 177–189. DOI: [10.1016/S0009-2797\(00\)00143-5](https://doi.org/10.1016/S0009-2797(00)00143-5).

[31] Shutava, T. G.; Balkundi, S. S.; Vangala, P.; Steffan, J. J.; Bigelow, R. L.; Cardelli, J. A.; O’Neal, D. P.; Lvov, Y. M. Layer-by-Layer-Coated Gelatin Nanoparticles as a Vehicle for Delivery of Natural Polyphenols. *ACS Nano* **2009**, *3*, 1877–1885. DOI: [10.1021/nn900451a](https://doi.org/10.1021/nn900451a).

[32] Isenburg, J. C.; Simionescu, D. T.; Vyawahare, N. R. Elastin Stabilization in Cardiovascular Implants: Improved Resistance to Enzymatic Degradation by Treatment with Tannic Acid. *Biomaterials* **2004**, *25*, 3293–3302. DOI: [10.1016/j.biomaterials.2003.10.001](https://doi.org/10.1016/j.biomaterials.2003.10.001).

[33] Shukla, A.; Fang, J. C.; Puranam, S.; Jensen, F. R.; Hammond, P. T. Hemostatic Multilayer Coatings. *Adv. Mater.* **2012**, *24*, 492–496. DOI: [10.1002/adma.201103794](https://doi.org/10.1002/adma.201103794).

[34] Van Buren, J. P.; Robinson, W. B. Formation of Complexes between Protein and Tannic Acid. *J. Agric. Food Chem.* **1969**, *17*, 772–777. DOI: [10.1021/jf60164a003](https://doi.org/10.1021/jf60164a003).

[35] Fan, H.; Wang, L.; Feng, X.; Bu, Y.; Wu, D.; Jin, Z. Supramolecular Hydrogel Formation Based on Tannic Acid. *Macromolecules* **2017**, *50*, 666–676. DOI: [10.1021/acs.macromol.6b02106](https://doi.org/10.1021/acs.macromol.6b02106).

[36] Erel-Unal, I.; Sukhishvili, S. A. Hydrogen-Bonded Multilayers of a Neutral Polymer and a Polyphenol. *Macromolecules* **2008**, *41*, 3962–3970. DOI: [10.1021/ma800186q](https://doi.org/10.1021/ma800186q).

[37] Shin, M.; Kim, K.; Shim, W.; Yang, J. W.; Lee, H. Tannic Acid as a Degradable Mucoadhesive Compound. *ACS Biomater. Sci. Eng.* **2016**, *2*, 687–696. DOI: [10.1021/acsbiomaterials.6b00051](https://doi.org/10.1021/acsbiomaterials.6b00051).

[38] Wu, L.; Hoa, S. V.; Ton-That, M. T. Effects of Water on the Curing and Properties of Epoxy Adhesive Used for Bonding FRP Composite Sheet to Concrete. *J. Appl. Polym. Sci.* **2004**, *92*, 2261–2268. DOI: [10.1002/app.20195](https://doi.org/10.1002/app.20195).

[39] Dizon, R. M.; Edwards, A. J.; Gomez, E. D. Comparison of Three Types of Adhesives in Attaching Coral Transplants to Clam Shell Substrates. *Aquat. Conserv. Mar. Freshw. Ecosyst.* **2007**, *656*, 636–656. DOI: [10.1002/aqc](https://doi.org/10.1002/aqc).

[40] Lee, D.; Hwang, H.; Kim, J. S.; Park, J.; Youn, D.; Kim, D.; Hahn, J.; Seo, M.; Lee, H. VATA: A Poly(Vinyl Alcohol)- and Tannic Acid-Based Nontoxic Underwater Adhesive. *ACS Appl. Mater. Interfaces* **2020**, *12*, 20933–20941. DOI: [10.1021/acsami.0c02037](https://doi.org/10.1021/acsami.0c02037).

[41] Fan, H.; Wang, J.; Zhang, Q.; Jin, Z. Tannic Acid-Based Multifunctional Hydrogels with Facile Adjustable Adhesion and Cohesion Contributed by Polyphenol Supramolecular Chemistry. *ACS Omega* **2017**, *2*, 6668–6676. DOI: [10.1021/acsomega.7b01067](https://doi.org/10.1021/acsomega.7b01067).

[42] Sanandiya, N. D.; Lee, S.; Rho, S.; Lee, H.; Kim, I. S.; Hwang, D. S. Tunichrome-Inspired Pyrogallol Functionalized Chitosan for Tissue Adhesion and Hemostasis. *Carbohydr. Polym.* **2019**, *208*, 77–85. (December 2018), DOI: [10.1016/j.carbpol.2018.12.017](https://doi.org/10.1016/j.carbpol.2018.12.017).

[43] Han, N.; Xu, Z.; Cui, C.; Li, Y.; Zhang, D.; Xiao, M.; Fan, C.; Wu, T.; Yang, J.; Liu, W. A Fe<sup>3+</sup>-Crosslinked Pyrogallol-Tethered Gelatin Adhesive Hydrogel with Antibacterial Activity for Wound Healing. *Biomater. Sci.* **2020**, *8*, 3164–3172. DOI: [10.1039/d0bm00188k](https://doi.org/10.1039/d0bm00188k).

[44] Samanta, S.; Rangasami, V. K.; Murugan, N. A.; Parihar, V. S.; Varghese, O. P.; Oommen, O. P. An Unexpected Role of an Extra Phenolic Hydroxyl on the Chemical Reactivity and Bioactivity of Catechol or Gallol Modified Hyaluronic Acid Hydrogels. *Polym. Chem.* **2021**, *12*, 2987–2991. DOI: [10.1039/D1PY00013F](https://doi.org/10.1039/D1PY00013F).

[45] Gwak, M. A.; Hong, B. M.; Seok, J. M.; Park, S. A.; Park, W. H. Effect of Tannic Acid on the Mechanical and Adhesive Properties of Catechol-Modified Hyaluronic Acid Hydrogels. *Int. J. Biol. Macromol.* **2021**, *191*, 699–705. DOI: [10.1016/j.ijbiomac.2021.09.123](https://doi.org/10.1016/j.ijbiomac.2021.09.123).

[46] Chen, K.; Lin, Q.; Wang, L.; Zhuang, Z.; Zhang, Y.; Huang, D.; Wang, H. An All-in-One Tannic Acid-Containing Hydrogel Adhesive with High Toughness, Notch Insensitivity, Self-Healability, Tailorable Topography, and Strong, Instant, and on-Demand Underwater Adhesion. *ACS Appl. Mater. Interfaces* **2021**, *13*, 9748–9761. DOI: [10.1021/acsami.1c00637](https://doi.org/10.1021/acsami.1c00637).

[47] Gu, W.; Liu, X.; Li, F.; Shi, S. Q.; Xia, C.; Zhou, W.; Zhang, D.; Gong, S.; Li, J. Tough, Strong, and Biodegradable Composite Film with Excellent UV Barrier Performance Comprising Soy Protein Isolate, Hyperbranched Polyester, and Cardanol Derivative. *Green Chem.* **2019**, *21*, 3651–3665. DOI: [10.1039/C9GC01081E](https://doi.org/10.1039/C9GC01081E).

[48] Wang, Z.; Kang, H.; Liu, H.; Zhang, S.; Xia, C.; Wang, Z.; Li, J. Dual-Network Nanocross-Linking Strategy to Improve Bulk Mechanical and Water-Resistant Adhesion Properties of Biobased Wood Adhesives. *ACS Sustain. Chem. Eng.* **2020**, *8*, 16430–16440. DOI: [10.1021/acssuschemeng.0c04913](https://doi.org/10.1021/acssuschemeng.0c04913).

[49] Xu, C.; Xu, Y.; Chen, M.; Zhang, Y.; Li, J.; Gao, Q.; Shi, S. Q. Soy Protein Adhesive with Bio-Based Epoxidized Daidzein for High Strength and Mildew Resistance. *Chem. Eng. J.* **2020**, *390*, (October 2019), 124622. DOI: [10.1016/j.cej.2020.124622](https://doi.org/10.1016/j.cej.2020.124622).

[50] Ma, C.; Pang, H.; Liu, H.; Yan, Q.; Li, J.; Zhang, S. A Tough, Adhesive, Self-Healable, and Antibacterial Plant-Inspired Hydrogel Based on Pyrogallol-Borax Dynamic Cross-Linking. *J. Mater. Chem. B* **2021**, *9*, 4230–4240. DOI: [10.1039/d1tb00763g](https://doi.org/10.1039/d1tb00763g).

[51] Gu, W.; Liu, X.; Ye, Q.; Gao, Q.; Gong, S.; Li, J.; Shi, S. Q. Bio-Inspired Co-Deposition Strategy of Aramid Fibers to Improve Performance of Soy Protein Isolate-Based Adhesive. *Ind. Crops Prod.* **2020**, *150*, 112424. DOI: [10.1016/j.indcrop.2020.112424](https://doi.org/10.1016/j.indcrop.2020.112424).

[52] Liu, H.; Geng, H.; Zhang, X.; Wang, X.; Hao, J.; Cui, J. Hot Melt Super Glue: Multi-Recyclable Polyphenol-Based Supramolecular Adhesives. *Macromol. Rapid Commun.* **2022**, *43*, 2100830–2100838. DOI: [10.1002/marc.202100830](https://doi.org/10.1002/marc.202100830).

[53] Yang, N.; Yuan, R.; You, D.; Zhang, Q.; Wang, J.; Xuan, H.; Ge, L. Gallol-Based Constant Underwater Coating Adhesives for Severe Aqueous Conditions. *Colloids Surfaces A Physicochem. Eng. Asp.* **2022**, *634*, 127948. DOI: [10.1016/j.colsurfa.2021.127948](https://doi.org/10.1016/j.colsurfa.2021.127948).

[54] Ghobril, C.; Grinstaff, M. W. The Chemistry and Engineering of Polymeric Hydrogel Adhesives for Wound Closure: A Tutorial. *Chem. Soc. Rev.* **2015**, *44*, 1820–1835. DOI: [10.1039/c4cs00332b](https://doi.org/10.1039/c4cs00332b).

[55] Sun, C.; Luo, J.; Jia, T.; Hou, C.; Li, Y.; Zhang, Q.; Wang, H. Water-Resistant and Underwater Adhesive Ion-Conducting Gel for Motion-Robust Bioelectric Monitoring. *Chem. Eng. J.* **2022**, *431*, 134012. DOI: [10.1016/j.cej.2021.134012](https://doi.org/10.1016/j.cej.2021.134012).

[56] Mandell, S. P.; Gibran, N. S. Fibrin Sealants: Surgical Hemostat, Sealant and Adhesive. *Expert Opin. Biol. Ther.* **2014**, *14*, 821–830. DOI: [10.1517/14712598.2014.897323](https://doi.org/10.1517/14712598.2014.897323).

[57] Mansuri, S.; Kesharwani, P.; Jain, K.; Tekade, R. K.; Jain, N. K. Mucoadhesion: A Promising Approach in Drug Delivery System. *React. Funct. Polym.* **2016**, *100*, 151–172. DOI: [10.1016/j.reactfunctpolym.2016.01.011](https://doi.org/10.1016/j.reactfunctpolym.2016.01.011).

[58] Yang, Q.; Tang, L.; Guo, C.; Deng, F.; Wu, H.; Chen, L.; Huang, L.; Lu, P.; Ding, C.; Ni, Y.; Zhang, M. A Bioinspired Gallol-Functionalized Collagen as Wet-Tissue Adhesive for Biomedical Applications. *Chem. Eng. J.* **2021**, *417*, 127962. DOI: [10.1016/j.cej.2020.127962](https://doi.org/10.1016/j.cej.2020.127962).

[59] Peng, Q.; Wu, Q.; Chen, J.; Wang, T.; Wu, M.; Yang, D.; Peng, X.; Liu, J.; Zhang, H.; Zeng, H. Coacervate-Based Instant and Repeatable Underwater Adhesive with Anticancer and Antibacterial Properties. *ACS Appl. Mater. Interfaces* **2021**, *13*, 48239–48251. DOI: [10.1021/acsami.1c13744](https://doi.org/10.1021/acsami.1c13744).

[60] Lee, J. S.; Cho, J. H.; An, S.; Shin, J.; Choi, S.; Jeon, E. J.; Cho, S. W. In Situ Self-Cross-Linkable, Long-Term Stable Hyaluronic Acid Filler by Gallol Autoxidation for Tissue Augmentation and Wrinkle Correction. *Chem. Mater.* **2019**, *31*, 9614–9624. DOI: [10.1021/acs.chemmater.9b02802](https://doi.org/10.1021/acs.chemmater.9b02802).

[61] Vasis, J. K.; Tambwekar, K.; Garg, S. Bioadhesive Microspheres as a Controlled Drug Delivery System. *Int. J. Pharm.* **2003**, *255*, 13–32. DOI: [10.1016/S0378-5173\(03\)00087-5](https://doi.org/10.1016/S0378-5173(03)00087-5).

[62] Cho, J. H.; Lee, J. S.; Shin, J.; Jeon, E. J.; An, S.; Choi, Y. S.; Cho, S. W. Ascidian-Inspired Fast-Forming Hydrogel System for Versatile Biomedical Applications: Pyrogallol Chemistry for Dual Modes of Crosslinking Mechanism. *Adv. Funct. Mater.* **2018**, *28*, 1705244–1705210. DOI: [10.1002/adfm.201705244](https://doi.org/10.1002/adfm.201705244).

[63] Lee, H. A.; Shin, M.; Kim, J.; Choi, J. W.; Lee, H. Designing Adaptive Binders for Microenvironment Settings of Silicon Anode Particles. *Adv. Mater.* **2021**, *33*, 2007460. DOI: [10.1002/adma.202007460](https://doi.org/10.1002/adma.202007460).

[64] Nemani, S. K.; Annavarapu, R. K.; Mohammadian, B.; Raiyan, A.; Heil, J.; Haque, A.; Abdelaal, A.; Sojoudi, H. Surface Modification of Polymers : Methods and Applications. *Adv.*

[65] *Mater. Interfaces* **2018**, *5*, 1801247–1801226. DOI: [10.1002/admi.201801247](https://doi.org/10.1002/admi.201801247).

[66] Nady, N.; Franssen, M. C. R.; Zuilhof, H.; Mohy, M. S.; Boom, R.; Schroën, K. Modi Fi Cation Methods for Poly (Arylsulfone) Membranes : A Mini - Review Focusing on Surface Modi Fi Cation. *Desalination* **2011**, *275*, 1–9. DOI: [10.1016/j.desal.2011.03.010](https://doi.org/10.1016/j.desal.2011.03.010).

[67] Lee, H.; Scherer, N. F.; Messersmith, P. B. Single-Molecule Mechanics of Mussel Adhesion. *Proc. Natl. Acad. Sci. U.S.A.* **2006**, *103*, 12999–13003. DOI: [10.1073/pnas.0605552103](https://doi.org/10.1073/pnas.0605552103).

[68] Hlushko, H.; Cubides, Y.; Hlushko, R.; Kelly, T. M.; Castaneda, H.; Sukhishvili, S. A. Hydrophobic Antioxidant Polymers for Corrosion Protection of an Aluminum Alloy. *ACS Sustainable Chem. Eng.* **2018**, *6*, 14302–14313. DOI: [10.1021/acssuschemeng.8b02966](https://doi.org/10.1021/acssuschemeng.8b02966).

[69] Hlushko, R.; Hlushko, H.; Sukhishvili, S. A. A Family of Linear Phenolic Polymers with Controlled Hydrophobicity, Adsorption and Antioxidant Properties. *Polym. Chem.* **2018**, *9*, 506–516. DOI: [10.1039/C7PY01973D](https://doi.org/10.1039/C7PY01973D).

[70] Chung, J. H. Y.; Naficy, S.; Yue, Z.; Kapsa, R.; Quigley, A.; Moulton, S. E.; Wallace, G. G. Bio-Ink Properties and Printability for Extrusion Printing Living Cells. *Biomater. Sci.* **2013**, *1*, 763–773. DOI: [10.1039/C3BM00012E](https://doi.org/10.1039/C3BM00012E).

[71] Shin, M.; Galarraga, J. H.; Kwon, M. Y.; Lee, H.; Burdick, J. A. Gallo-Derived ECM-Mimetic Adhesive Bioinks Exhibiting Temporal Shear-Thinning and Stabilization Behavior. *Acta Biomater.* **2019**, *95*, 165–175. DOI: [10.1016/j.actbio.2018.10.028](https://doi.org/10.1016/j.actbio.2018.10.028).

[72] Rahim, M. A.; Centurion, F.; Han, J.; Abbasi, R.; Mayyas, M.; Sun, J.; Christoe, M. J.; Esrafilzadeh, D.; Allioux, F.; Ghasemian, M. B.; et al. Polyphenol-Induced Adhesive Liquid Metal Inks for Substrate-Independent Direct Pen Writing. *Adv. Funct. Mater.* **2021**, *31*, 2007336. DOI: [10.1002/adfm.202007336](https://doi.org/10.1002/adfm.202007336).

[73] Wu, Y.; Deng, Z.; Peng, Z.; Zheng, R.; Liu, S.; Xing, S.; Li, J.; Huang, D.; Liu, L. A Novel Strategy for Preparing Stretchable and Reliable Biphasic Liquid Metal. *Adv. Funct. Mater.* **2019**, *29*, 1903840. DOI: [10.1002/adfm.201903840](https://doi.org/10.1002/adfm.201903840).

[74] Joshipura, I. D.; Ayers, H. R.; Majidi, C.; Dickey, M. D. Methods to Pattern Liquid Metals. *J. Mater. Chem. C* **2015**, *3*, 3834–3841. DOI: [10.1039/C5TC00330J](https://doi.org/10.1039/C5TC00330J).

[75] Boley, J. W.; White, E. L.; Chiu, G. T.; Kramer, R. K. Direct Writing of Gallium-Indium Alloy for Stretchable Electronics. *Adv. Funct. Mater.* **2014**, *24*, 3501–3507. DOI: [10.1002/adfm.201303220](https://doi.org/10.1002/adfm.201303220).